

MARIANA NATALE FIORELLI FABICHE
(ORGANIZER)

ENGINEERING IN PERSPECTIVE

SCIENCE, TECHNOLOGY
AND INNOVATION

Atena
Editora
2024

MARIANA NATALE FIORELLI FABICHE
(ORGANIZER)

ENGINEERING IN PERSPECTIVE

SCIENCE, TECHNOLOGY
AND INNOVATION

Atena
Editora
2024

Chief editor

Profª Drª Antonella Carvalho de Oliveira

Executive editor

Natalia Oliveira

Editorial assistant

Flávia Roberta Barão

Librarian

Janaina Ramos

Graphic project

Ellen Andressa Kubisty

Luiza Alves Batista

Nataly Evilin Gayde

Thamires Camili Gayde

Cover pictures

iStock

Art edition

Luiza Alves Batista

2024 by Atena Editora

Copyright © Atena Editora

Copyright of the text © 2024 The authors

Copyright of the edition © 2024 Atena Editora

Rights for this edition granted to Atena Editora by the authors.

Open access publication by Atena Editora



All content in this book is licensed under a Creative Commons Attribution License. Attribution-Non-Commercial-NonDerivatives 4.0 International (CC BY-NC-ND 4.0).

The content of the articles and their data in their form, correctness and reliability are the sole responsibility of the authors, and they do not necessarily represent the official position of Atena Editora. It is allowed to download the work and share it as long as credits are given to the authors, but without the possibility of altering it in any way or using it for commercial purposes.

All manuscripts were previously submitted to blind evaluation by peers, members of the Editorial Board of this Publisher, having been approved for publication based on criteria of academic neutrality and impartiality.

Atena Editora is committed to ensuring editorial integrity at all stages of the publication process, avoiding plagiarism, fraudulent data or results and preventing financial interests from compromising the publication's ethical standards. Suspected scientific misconduct situations will be investigated to the highest standard of academic and ethical rigor.

Editorial Board**Exact and earth sciences and engineering**

Prof. Dr. Adélio Alcino Sampaio Castro Machado – Universidade do Porto

Profª Drª Alana Maria Cerqueira de Oliveira – Instituto Federal do Acre

Profª Drª Ana Grasielle Dionísio Corrêa – Universidade Presbiteriana Mackenzie

Profª Drª Ana Paula Florêncio Aires – Universidade de Trás-os-Montes e Alto Douro

Prof. Dr. Carlos Eduardo Sanches de Andrade – Universidade Federal de Goiás

Profª Drª Carmen Lúcia Voigt – Universidade Norte do Paraná

Prof. Dr. Cleiseano Emanuel da Silva Paniagua – Colégio Militar Dr. José Aluisio da Silva Luz / Colégio Santa Cruz de Araguaia/TO

Profª Drª Cristina Aledi Felseburgh – Universidade Federal do Oeste do Pará

Prof. Dr. Diogo Peixoto Cordova – Universidade Federal do Pampa, Campus Caçapava do Sul

Prof. Dr. Douglas Gonçalves da Silva – Universidade Estadual do Sudoeste da Bahia

Prof. Dr. Eloi Rufato Junior – Universidade Tecnológica Federal do Paraná

Profª Drª Érica de Melo Azevedo – Instituto Federal do Rio de Janeiro

Prof. Dr. Fabrício Menezes Ramos – Instituto Federal do Pará

Prof. Dr. Fabrício Moraes de Almeida – Universidade Federal de Rondônia

Profª Drª Glécilla Colombelli de Souza Nunes – Universidade Estadual de Maringá

Prof. Dr. Hauster Maximiler Campos de Paula – Universidade Federal de Viçosa

Profª Drª Iara Margolis Ribeiro – Universidade Federal de Pernambuco

Profª Drª Jéssica Barbosa da Silva do Nascimento – Universidade Estadual de Santa Cruz

Profª Drª Jéssica Verger Nardeli – Universidade Estadual Paulista Júlio de Mesquita Filho

Prof. Dr. Juliano Bitencourt Campos – Universidade do Extremo Sul Catarinense

Prof. Dr. Juliano Carlo Rufino de Freitas – Universidade Federal de Campina Grande

Prof. Dr. Leonardo França da Silva – Universidade Federal de Viçosa

Profª Drª Luciana do Nascimento Mendes – Instituto Federal de Educação, Ciência e Tecnologia do Rio Grande do Norte

Prof. Dr. Marcelo Marques – Universidade Estadual de Maringá

Prof. Dr. Marco Aurélio Kistemann Junior – Universidade Federal de Juiz de Fora

Prof. Dr. Marcos Vinicius Winckler Caldeira – Universidade Federal do Espírito Santo

Profª Drª Maria Iaponeide Fernandes Macêdo – Universidade do Estado do Rio de Janeiro

Profª Drª Maria José de Holanda Leite – Universidade Federal de Alagoas

Profª Drª Mariana Natale Fiorelli Fabiche – Universidade Estadual de Maringá

Prof. Dr. Miguel Adriano Inácio – Instituto Nacional de Pesquisas Espaciais

Prof. Dr. Milson dos Santos Barbosa – Universidade Tiradentes

Profª Drª Natiéli Piovesan – Instituto Federal do Rio Grande do Norte

Profª Drª Neiva Maria de Almeida – Universidade Federal da Paraíba

Prof. Dr. Nilzo Ivo Ladwig – Universidade do Extremo Sul Catarinense

Profª Drª Priscila Natasha Kinas – Universidade do Estado de Santa Catarina

Profª Drª Priscila Tessmer Scaglioni – Universidade Federal de Pelotas

Prof. Dr. Rafael Pacheco dos Santos – Universidade do Estado de Santa Catarina

Prof. Dr. Ramiro Picoli Nippes – Universidade Estadual de Maringá

Profª Drª Regina Célia da Silva Barros Allil – Universidade Federal do Rio de Janeiro

Prof. Dr. Sidney Gonçalo de Lima – Universidade Federal do Piauí

Prof. Dr. Takeshy Tachizawa – Faculdade de Campo Limpo Paulista

Engineering in perspective: science, technology and innovation

Diagramming: Ellen Addressa Kubisty
Correction: Maiara Ferreira
Indexing: Amanda Kelly da Costa Veiga
Review: The authors
Organizer: Mariana Natale Fiorelli Fabiche

International Cataloging-in-Publication Data (CIP)	
E57	Engineering in perspective: science, technology and innovation / Organizer Mariana Natale Fiorelli Fabiche. – Ponta Grossa - PR: Atena, 2024. Formato: PDF Requisitos de sistema: Adobe Acrobat Reader Modo de acesso: World Wide Web Inclui bibliografia ISBN 978-65-258-2559-5 DOI: https://doi.org/10.22533/at.ed.595241305 1. Engineering. I. Fabiche, Mariana Natale Fiorelli (Organizer). II. Title. CDD 620
Prepared by Librarian Janaina Ramos – CRB-8/9166	

Atena Editora
Ponta Grossa – Paraná – Brasil
Telefone: +55 (42) 3323-5493
www.atenaeditora.com.br
contato@atenaeditora.com.br

AUTHORS' DECLARATION

The authors of this work: 1. Attest that they do not have any commercial interest that constitutes a conflict of interest in relation to the published scientific article; 2. They declare that they actively participated in the construction of their manuscripts, preferably in: a) Study design, and/or data acquisition, and/or data analysis and interpretation; b) Elaboration of the article or revision in order to make the material intellectually relevant; c) Final approval of the manuscript for submission; 3. They certify that published scientific articles are completely free from fraudulent data and/or results; 4. Confirm correct citation and reference of all data and interpretations of data from other research; 5. They acknowledge having informed all sources of funding received for carrying out the research; 6. Authorize the publication of the work, which includes the catalog records, ISBN (Internacional Standard Serial Number), D.O.I. (Digital Object Identifier) and other indexes, visual design and cover creation, interior layout, as well as the release and dissemination according to Atena Editora's criteria.

PUBLISHER'S DECLARATION

Atena Editora declares, for all legal purposes, that: 1. This publication constitutes only a temporary transfer of copyright, right to publication, and does not constitute joint and several liability in the creation of published manuscripts, under the terms provided for in the Law on Rights copyright (Law 9610/98), in art. 184 of the Penal Code and in art. 927 of the Civil Code; 2. Authorizes and encourages authors to sign contracts with institutional repositories, with the exclusive purpose of disseminating the work, provided that with due acknowledgment of authorship and editing and without any commercial purpose; 3. All e-books are open access, so it does not sell them on its website, partner sites, e-commerce platforms, or any other virtual or physical means, therefore, it is exempt from copyright transfers to authors; 4. All members of the editorial board are PhDs and linked to public higher education institutions, as recommended by CAPES for obtaining the Qualis book; 5. It does not transfer, commercialize or authorize the use of the authors' names and e-mails, as well as any other data from them, for any purpose other than the scope of dissemination of this work.

It is with great enthusiasm and dedication that I present to you, reader, the new collection “Engineering in perspective science, technology and innovation”. A collection of scientific works that addresses current and highlighted topics in the field of Engineering.





This consists of four chapters, covering various subjects carried out in various teaching and research institutions abroad in Brazil. Relevant issues such as the potential for reusing slate waste in the ceramics industry; the Integration of E-learning in the metaverse for the development of teaching and training in higher education; Thermal study of a coated oxygen for the production of hydrogen, as well as thermal-hydraulic advances in the production of this material.

A new, current and contemporary collection, aiming to provide learning opportunities for readers in both the academic and professional fields. Furthermore, this work seeks to encourage the dissemination of new work and highlights the importance of researchers in publishing their work through reliable platforms, such as Atena Editora.

To the authors, I thank you for your trust and spirit of partnership.

Good Reading

Mariana Natale Fiorelli Fabiche

CHAPTER 1.....	1
EXPLORING THE POTENTIAL REUSE OF SLATE WASTE IN THE CERAMIC INDUSTRY: A CONTRIBUTION TO CIRCULAR ECONOMY AND ENVIRONMENTAL CONSERVATION	
Luciana B. Palhares	
Cláudio G dos Santos	
Pollyanna Aparecida da S. Araújo	
Rafael Vasconcelos S. Lopes	
Vinícius M. Torres	
 https://doi.org/10.22533/at.ed.5952413051	
CHAPTER 2	14
INTEGRATING E-LEARNING IN METAVERSE FOR SUSTAINABLE DEVELOPMENT OF HIGHER EDUCATION AND TRAINING	
Nguyen Duc Son	
 https://doi.org/10.22533/at.ed.5952413052	
CHAPTER 3	24
THERMAL PERFORMANCE OF A JACKETED MULTIPHASE OXYGEN REACTORS IN THE COPPER CHLORINE CYCLE FOR HYDROGEN PRODUCTION	
Mohammed Wassef Abdulrahman	
 https://doi.org/10.22533/at.ed.5952413053	
CHAPTER 4	44
ADVANCES IN THERMAL HYDRAULICS OF OXYGEN PRODUCTION REACTORS IN THE COPPER-CHLORINE CYCLE FOR HYDROGEN PRODUCTION: A COMPREHENSIVE REVIEW	
Mohammed Wassef Abdulrahman	
 https://doi.org/10.22533/at.ed.5952413054	
ABOUT THE ORGANIZER	69
INDEX.....	70

EXPLORING THE POTENTIAL REUSE OF SLATE WASTE IN THE CERAMIC INDUSTRY: A CONTRIBUTION TO CIRCULAR ECONOMY AND ENVIRONMENTAL CONSERVATION

Acceptance date: 02/05/2024

Luciana B. Palhares

Departamento de Engenharia de
Materiais, CEFET-MG, Belo Horizonte,
MG, Brazil
<https://orcid.org/0000-0001-6887-9101>

Cláudio G dos Santos

Departamento de Engenharia de
Materiais, CEFET-MG, Belo Horizonte,
MG, Brazil

Pollyanna Aparecida da S. Araújo

Departamento de Engenharia de
Materiais, CEFET-MG, Belo Horizonte,
MG, Brazil
Departamento de Química, UFOP, CEP
35400-000, Ouro Preto, MG, Brazil

Rafael Vasconcelos S. Lopes

Departamento de Engenharia de
Materiais, CEFET-MG, Belo Horizonte,
MG, Brazil

Vinícius M. Torres

Departamento de Engenharia de
Materiais, CEFET-MG, Belo Horizonte,
MG, Brazil

of generating significant amounts of waste, impacting sustainability and environmental conservation. The present study aimed to investigate the feasibility of using slate waste in ceramic processing, specifically through slip-casting techniques. By conducting detailed experimental procedures and characterization tests, the study seeks to provide insights into the suitability of slate waste as a substitute for conventional raw materials. Additionally, the study aimed to evaluate the technical properties and performance of ceramic pieces produced using slate waste, thereby addressing concerns about the quality and applicability of such materials in practical applications. Slate rejects collected from quarries were characterized and ceramic pieces were produced by slip casting. The cast green and sintered samples were characterized by density, pore size distribution by mercury porosity, surface area evaluation, X-ray diffraction techniques, and scanning electron microscopy. The X-ray results, when confronted with thermal analyses, have shown major structural transitions at approximately 550°C and 850°C. The studies of porosity and density of pieces, before and after heat treatment, provided a better understanding of the slate sintering

ABSTRACT: Throughout the years, mining activity has had great importance for economic progress, despite its repercussions

process. The results indicate that the density decreases after heat treatment and the pieces show a volume reduction due to slate reactions. Compacts formed by slip-casting different suspensions showed an average pore size of approximately 0.72 mm, suggesting that the structural changes that occurred in the slate greatly influenced the porosities and densities of the resulting materials. The results allow us to infer that slate powder from rejects has a great potential for being recovered, recycled, and applied in ceramic processing, producing various ceramic products. These products encompass a wide range of applications, including but not limited to sanitary ware, decorative pieces, and architectural elements.

KEYWORDS: Slate waste, Material reuse, Recycling, Ceramic processing, Sustainability.

INTRODUCTION

Different society segments have been devoting attention to slate waste treatment techniques and recycling, especially universities, tech institutes, and industries, focusing on the massive amount of waste produced in its extraction sites. These rejects are almost always incorrectly disposed of by the respective companies, contributing to environmental degradation.

Brazil is accounted for its varied geodiversity, supporting its worldwide importance as an exporter of ornamental rocks. Truly, the country is the third largest slate producer and exporter, with the state of Minas Gerais accounting for about 90% of this production (approximately 0.4 million tons/year) and almost all Brazilian exports. Slate derivatives from Minas Gerais unfold into approximately 18 million square meters of slabs, tiles, pool countertops, roofs, and other products, according to Abirochas (2018). The natural slate extraction, cutting, and polishing process is extremely wasteful and its reject stream from quarrying is not properly managed in the present day. According to Oti, Kinuthia and Bai (2010) finished pieces derived from slate have shape and size requirements that make it unfeasible to use all extracted raw material, so only around 10% end up entering the production process, and even less reach the final phases. Frias *et al.* (2014) report that slate used in civil construction generates between 75% and 90% in weight of waste, and one possible way of reusing it is through thermal activation and manufacturing new cementitious materials. The large amounts of engendered slate waste happen because of many variables: poor extractive and processing activity technological profile; research deficiency on qualifying new mining fronts; lack of boulder-type slate exploitation; resistance to directing sales to the foreign market as long as the domestic one, which would be more profitable allied to public-private partnerships to promote less bureaucratic processes, to name a few. All of those result in an excessive quantity of rejects – small pieces of irregularly shaped or liquid-effluent rocks, and also mud from cutting and polishing processes (Palhares, Santos and Hunter, 2016).

The waste produced annually by Brazilian slate industries is nearly 0.3 million tons (Oti, Kinuthia and Bai, 2010). It is composed mainly of water, lubricants, crushed rock, and

slate fragments. The production of alternative materials with the slate waste brought as a constituent to the rock manufacturing industries may reduce or even eliminate pollution in the extraction areas, aside from promoting new job opportunities and income – essential to the country's progress and development. Many studies have reported the production of new materials with slate waste through traditional ceramic processes, such as pressing, extrusion, slip casting, and others. In Palhares *et al*, (1997) work, there were several slate bricks produced by pressing and heat-treating the samples up to 1000°C. Their compressive strength tests showed that bricks have great potential for use in civil construction. Catarino *et al*. (2003) used residue powders from cutting and machining operations in slate quarries to produce flooring and roofing tiles by a press (at 40 MPa) and sintering route (up to 1150 °C). The authors showed that the properties of the products obtained were suitable for flooring tiles. Cambroner, Ruiz-Roman and Ruiz-Pietro (2005) obtained foams (porous ceramic) without any foaming agent addition and, according to them, the resulting material reaches adequate strength after the transformations suffered by the slate components during heating. Silva and Peres (2006) investigated the pozzolanicity of slate wastes and confirmed such activity with calcinated slate samples but not with natural ones. They proposed the use of slate wastes in the cement industry as mineral addition in partial substitution to Portland cement clinker. Snelson *et al*. (2010) reviewed the potential of using slate waste and suggested the great potential for using slate waste in many situations, including engineering applications despite reported transportation difficulties. Generally, the use of slate wastes is feasible and could minimize the environmental impact of their disposal but in countries with a large territorial area such as Brazil, without an adequate railway network, this transport can increase costs and make their use impracticable for ceramic industries. Zhen, *et al*, (2018) processed the slate wastes to form ceramsite slate, a kind of artificial foam, similar to that obtained by Cambroner, Ruiz-Roma and Ruiz-Pietro (2005). The ultra-light ceramsite could be directly used as building aggregate since its properties were shown to be superior to other ceramsites. At present, mercury intrusion porosimetry (MIP) is still today the reference experimental method to obtain the pore size distribution of dry samples of porous media (Cieszko, Kempinski and Czerwinski, 2019), despite its environmental health and safety concerns. Some substantial benefits of this extensively used technique include the relatively fast measurements, the possibility of covering a large range of pore sizes, i.e., from 10^{-9} up to 10^{-3} m (Zhang, *et al*, (2016), and the richness of accessible databases.

In the present work, the utilization of slate waste in ceramic processing was examined, emphasizing its feasibility as an alternative resource and its potential contributions to sustainability and resource conservation. This initiative aimed to enhance economic efficiency while concurrently addressing the issue of overexploitation of clay quarries. The pore structure of ceramic pieces manufactured via slip casting was evaluated. Characterization tests, utilizing Mercury Intrusion Porosimetry (MIP) techniques, were conducted before and

after burning to investigate morphology modifications and pore structure changes during thermal treatment.

EXPERIMENTAL PROCEDURE

The slate powder used in this work was kindly donated by the Company Micapel Slate, located in the city of Pompeu, state of Minas Gerais, and was produced via block extraction for the production of slabs, floors, and roofs.

It was pre-treated before characterization to remove impurities such as organic waste and lubrication contamination. The steps of this treatment were: preparing for powder suspension in distilled water, wet sieving with the #400 sieve; 24-hour decanting; siphonation (water removal), and oven drying at 120°C for 24 hours.

Powder composition and crystallinity were determined with a diffractometer XRD Philips - X-Ray Generator, No. DY 1308, type PW 1730/10 with Cu-K_α rad radiation, 35kV, goniometer speed of 0,02°/min in 2θ per step, with a 5 seconds per step time count and collection from 5° to 80° in 2θ. For the refinement, the General Structure Analysis System Program (Larson and Von Dreele, 2001) was employed with the EXPGUI interface, using the Thompson-Cox-Hastings pseudo-Voigt profile function, with background radiation adjusted by the Chebyshev polynomial. The mineralogical analysis of the slate powder was obtained through refinement by the Rietveld method. The adjustment parameters c2, R_p, and R_{wp} for the analyzed samples were 5.5%, 5.6%, and 6.6%, respectively. The semi-quantitative analyses were carried out on a Shimadzu 7000, model EDX-720 equipment.

SEM images were obtained with a Scanning Electron Microscope LEO/Zeiss 1530 (LEO Elektronmikroskope GmbH, Germany) joined with energy dispersive spectroscopy (EDS). The slate particles were suspended in water and a few drops of these suspensions were added to the stub and dried at 60°C. After that, the samples were uniformly coated with gold.

Thermogravimetric analyses were performed on a Shimadzu TA 50-WSI heat analyzer. The analysis was carried out in the temperature range of 20 °C–1150 °C with a heating rate of 10 K min⁻¹ under air atmosphere. The slate powder suspensions in distilled water were prepared with solids percentages varying from 48%w/v to 78%w/v (suspensions 1 to 3) and homogenized with a magnetic stirrer for 24 hours. Ammonium polyacrylate (purity degree – 98%) was used as a dispersant (varying from 1%v/v to 2.5%v/v – suspensions 4-6) and poly (vinyl alcohol) as a binder (purity degree – 99.8%, varying from 1%v/v to 2.5%v/v – suspensions 7-9); both chemicals were purchased from Aldrich and used as received.

For the manufacture of plaster molds, preforms were used and cut into sizes of about 2 inches in length. The molds were obtained with plaster to water ratio of 70 (100 g gypsum to 70 mL of water), and the mixture was stirred for 1 minute and poured into the pre-mold

to form the wish piece structure. After curing the mold, it was dried at room temperature for 15 days before use.

After casting, the pieces were dried at room temperature for 24 hours, followed by oven heating at 100°C and finally heat-treated in an electric furnace at the temperatures 500°C, 700°C, 1000°C, 1050°C and 1100°C with a 10°C/min heating rate in air. The green sample is generally referred to as “cast” since it is measured before heat treatment. The *as-cast* and after-sintering densities were determined by a helium pycnometer (Multipycnometer – Quantachrome). The Auto Pore III 9420 (Micromeritics) was used to measure the mercury penetration porosimetry, for determining pore size distributions. Both low-pressure (0 to 345 kPa) and high-pressure (345 MPa to 414 MPa) penetration volumes were measured and collected automatically. A computer program was used to combine the low-pressure and high-pressure data and to convert the volume-pressure data to volume-diameter data. The BET method (Autosorb-1, Quantachrome), based on the N₂ adsorption model (at 77 K), was used to evaluate the average surface area.

RESULTS AND DISCUSSION

Powder Characterization

SEM images of the slate powder (Figure 1) show agglomerated particles having sizes ranging from 10 to 30 μm. There were different shapes identified among the particles, isotropic and laminar, with the appearance of leaves or small plates due to the large variety of minerals present in the slate.

The density values found via helium pycnometer and surface area analysis via nitrogen adsorption were, respectively, 2.76 g.cm⁻³ and 12.3 m². g⁻¹.

EDX analysis of the powder indicated abundant contents of SiO₂ (61.6%), Al₂O₃ (16.6%), K₂O (10.8%) and Fe₂O₃ (5.9%). These four oxides are the major constituents of slate. Catarino *et al.* (2003) found comparable values using the chemical analysis by FRX and reported the presence of 54.68% SiO₂, 9.95% Fe₂O₃, and 23.52% Al₂O₃. According to Cambronero, Ruiz-Roman and Ruiz-Pietro (2005) the chemical composition of the slate powder consists mainly of SiO₂ (50–60%) and Al₂O₃ (20–25%) and the XRD analysis of the powder showed peaks corresponding to the following constituents: quartz, hematite, chlorite, and muscovite.

The XRD analysis of slate powder identified the components: (Q) Quartz - SiO₂ (29,6%), (C) Chlinochlorite (19,2%), (M) muscovite (29,0%), (A) Albite (14,5%), (Ca) Calcite (1.8%), and (O) Orthoclase (5,9%) with errors 0,5; 0,4;0,4;0,7;0,7;0,4 respectively.

Comparing the chemical and mineralogical analyses, it is generally observed that silica (SiO₂) is the dominant mineral present in quartz, phyllosilicates (micas and chlorites), and feldspars. Alumina (Al₂O₃) is mainly contained in phyllosilicates and, to a lesser extent,

in feldspars, the same way as sodium and potassium oxides. Part of the potassium is present in muscovite, and the magnesium oxides originate from the clinocllore and the magnesium calcite.

Brazilian slate samples reported elsewhere displayed values similar to those found in this work. The values were 26-30% quartz, 32-34% mica, 18-20% chlorite, 12-15% feldspar, and 0.5-1% carbonates. Campos, Velasco e Martinez (2004), Chiodi Filho, Rodrigues e Arthur (2003) and Frias *et al.* (2014) also mention the presence of chamosite, quartz, muscovite, and feldspar.

The values obtained for the parameters c_2 , R_p , and R_{wp} refinements all fall within the range observed for natural multi-mineral systems, as demonstrated by Hill, Tsambourakis and Madsen (1993), Mumme *et al.* (1996) and Weidler *et al.* (1998).

The thermal analysis showed the main transitions of slate powder. At transition at 578°C, it may be assigned to the allotropic transformation of quartz and clinocllore and muscovite dihydroxylation. Around 740°C, the muscovite and clinocllore elements lose their lattice structure, and around 889°C, the calcite is decomposed. The mass losses associated with the described events were, respectively, 1.5%, 3.2%, 1.6%, and 0.87%.

Characterization of pieces

Table 1 shows the bulk density and volume reduction for the pieces obtained. Suspensions 1 to 3 confirm that when the solids percentage increase, the green density increases, due to the larger number of particulates in suspension, leading to less water release during the casting process. Conversely, when the dispersant percentage increased (suspensions 4 to 6), the green density decreased. This is explained by the particles being further apart, due to the increasing amount of dispersant used. When comparing the suspensions 1 to 3 with 4 to 6, the density found is higher in the latter set. In these cases, the dispersion is more effective inducing a slower deposition of the particle, which renders filling the empty spaces more effective, resulting in higher densities. This suggests that the binder could be competing with the dispersant in the surface particle, resulting in a less effective dispersion and an attraction between the slate particles, leading to lower densities. The use of the binder to obtain “as cast” pieces with adequate handling strength was adverse to the bonding process. For suspensions 7 to 9, the density is always higher than other suspensions due to the binder, which promotes particle bonding. By increasing the binder fraction, the green density decreases. It was also observed density reduction for all suspensions subsequently to the heat treatment.

When assessed, the density values were distant from the natural slate stone theoretical estimates, and these deviations could be caused by the thermal expansion of clinocllore and muscovite constituents. Along with it, there was an 8-10% weight loss caused by outgassing and volatile decomposition.

The pore distribution curves for the slate samples obtained through mercury porosimetry after casting, across all suspensions, reveal a tendency towards the macroporous range with a higher average size, corroborating with the density values.

The pore size distribution curves before and after heating of the suspensions prepared with different solids percentages and with constant dispersant and binder showed similar behavior. Before the heat treatment, the curves are not monomodal and the pore size range is relatively wide. The highest porosity range for green pieces is around 0.1 to 1mm. As the percentage of solids increased, the average pore diameter decreased from approximately 0.72 to 0.45mm, suggesting that the particle cluster was different and more efficient when the percentage of solids was increased. These values are consistent with the density growth, which in turn occurs along with the increase of solids percentage.

After the heat treatment, the distribution becomes relatively narrower and shifts to an average pore size of approximately 0.72 mm. This may be explained by crystal transitions and slate dihydroxylation. This process is not homogeneous, and it occurs in two steps. The first stage occurs at about 500°C and involves transitions related to interlayer water loss, whereas the second phase is caused by dihydroxylation and takes place at approximately 700°C (Guggenheim, Chang and Van-Gross, 1987). Furthermore, at high temperatures, changes in lattice structure could be taking place so that the tetrahedral sheets become hexagonal and fully extended onto their sides, resulting in structure expansion (Hazen, 1997).

For all samples, the porosity observed varied between 1 and 0.1 mm after the heat treatment. This suggests that changes in additive and solids percentages did not have an accentuated effect on the pore size distribution of the pieces and the structural transformations on the slate are primarily responsible for the bulk residual porosity. The thermal treatment reduces the total porosity but not quite the pores' size. These results are consistent with some clays that burn up to 1000°C and show a porosity increase as a result of the loss upon ignition, related to the decomposition of clay minerals and organic materials (Shu, *et al.*, 2012).

Usually, higher densities are related to smaller volume reductions; however, in this case, the green density is not the only factor influencing the volume shrinkage after the heat treatment. The structural changes that occurred in the slate at higher temperatures have a significant effect on the final properties of the ceramic pieces obtained through slip casting.

The structural changes describe the complex thermal transformations of the phase minerals of which the slate is formed. Many authors have studied the slate and reported its mineral reactions. Sanchez-Soto *et al.*, (2010) reported that chlorite and muscovite disappear at around 800°C and quartz is undragged, making this process exothermic. An increase in expansion up to 1020°C was interpreted by a bloating effect, caused by trapped gases in the pores and the release of oxygen gas, being the latter characteristic of raw materials containing iron oxides. All reactions promote a piece expansion, reducing the final density and increasing porosity.

According to Moura and Grade (1977) slate residual pores are due to the thermal expansion resulting from gases formation - CO_2 , SO_3 , and H_2O - accumulated in gas pockets, gases which are derived from the decomposition of organic matter, hydrous fine-grained phyllosilicates, such as illite, chlorite, muscovite, calcite, and hematite. Some of the evolved gases could become sealed inside the inorganic mass constituting the fired slate piece. The reactions that promote slate expansion take place within the temperature range of 400°C - 820°C , and essentially consist of the aforementioned evolved gases; from 820°C onwards the vitrification phase is initiated and progressively developed, resulting in the formation of an essentially alkaline alumino-silicate glass that provides gas retention in the most internal parts of black slate pieces. The slate expansion increases up to 1050°C - 1150°C , being the highest when the temperature reaches the maximum temperature value. As far as temperature increases and provides gas dilatation, this gas phase presses the glassy material that acquires and develops plasticity and elasticity. Gases can migrate up to the external surfaces of the slate pieces and escape to the kiln atmosphere (Costa, Almeida e Gomes, 2013).

The density and pore size of green compacts produced through slip casting are also influenced by the dispersion state of powder particles in suspension. The development of agglomerates may be controlled by adjusting the pH. Meanwhile, the dismantling of agglomerated particles may help obtain pieces with higher density and lower porosity. In addition, the thermal treatment at higher temperatures may form a liquid phase and fill the existing voids in the slate pieces, reducing the initially present porosity in the green fraction.

Table 1 shows the porosity of the samples before (green samples) and after heat treatment. As expected, all samples showed a porosity reduction after heat treatment. The remaining porosity is due to the structural modifications suffered by the slate, as discussed above.

The ceramic slate pieces' porosities presented a substantial value to all suspensions. Suspension 7 offered the best values, which can be associated with a more dispersed suspension and lower binder and dispersant concentrations, hence reducing agglomerates. In the case of suspensions formed by different minerals, their stability depends on each component's physicochemical surface characteristics. Their contribution depends on their relative quantity as well as their surface reactivity towards the other elements of the system. The minerals present in the slate have very different surface characteristics regarding their acidity/basicity concerning water. Therefore, it is inferred that suspension 7 was the most stable among those investigated in this work.

The series of SEM images in Figure 2 exhibits the microscopic evolution of the pieces obtained after heat treatment of suspension 7 at temperatures from 500°C to 1100°C . Figure 3 illustrates the corresponding evolution of the diffractograms.

From the SEM analysis, it was noticed that after burning, the samples acquired a smoother surface, making them less porous and stronger than the respective green pieces.

At elevated sintering temperatures, the presence of a liquid phase was perceived, but it was not enough to fill the pores (Costa, Almeida, and Gomes, 2013).

From X-ray diffraction results, it was possible to identify important reactions that occurred in slate pieces. New phases were identified, such as gehlenite, hercynite, and spinels. According to Binda *et al.* (2020), the presence of these minerals was anticipated, due to the presence of calcite in the raw material. The gehlenite is formed by reacting calcium oxide with Si and Al from the clay decomposition. At temperatures up to 500°C, the slate powder does not change. Starting at 700°C, the peaks referring to muscovite and clinocllore begin to disappear due to the release of structural water present in these minerals and the modifications in their crystalline structures. This observation is confirmed using differential thermal analysis with peaks between 700°C and 800°C. At temperatures above 1000°C, the presence of the amorphous phase is evidenced by the area under the peaks, due to a low-melting liquid phase formation (Palhares *et al.*, 2006).

The rise in temperature during the thermal process provides a reduction in surface area and the number of pores and voids (Table 2).

CONCLUSIONS

An experimental study was conducted to investigate the use of slate waste powder to produce ceramic pieces via the slip-casting process. It evaluated the influence of residue on the density and porosity of the pieces in temperatures until 1100oC.

Employing the slip-casting technique with slate waste as a raw material opens up avenues for the production of various ceramic products. These products encompass a wide range of applications, including but not limited to sanitary ware, decorative pieces, and architectural elements. The utilization of slate waste not only offers economic benefits but also contributes to sustainability by reducing the exploitation of clay quarries and facilitating the recovery of slate waste. By harnessing this alternative resource, the ceramic industry can diversify its product portfolio while minimizing its environmental footprint. The investigation underscores the potential of slate waste as a viable raw material in ceramic processing, highlighting its significance in promoting resource conservation and advancing sustainable practices within the industry.

The major constituents of slate powder were identified by X-ray diffraction as quartz, muscovite, and clinocllore not presenting different components of slate stone.

The studies of porosity and density of slate ceramic pieces, before and after heat treatment, provided a better understanding of the slate sintering process. The results indicate that the bulk density decreases after heat treatment and the pieces show a volume reduction due to slate reactions. Compacts formed by slip-casting different suspensions showed an average pore size of approximately 0.72 mm, suggesting that the structural changes that occurred in the slate greatly influenced the porosities and densities of the resulting materials.

Based on XRD results and thermal analysis of the slate samples and burned ceramic pieces, it was possible to identify several important alterations during the burn, which may have contributed to the porosity surge. Evaporation of free water, both physically and chemically adsorbed (at 250°C and 320°C, respectively), dihydroxylation of clays with the elimination of structural water (muscovite and clinocllore, 570°C–580°C), and calcite decomposition with CO₂ release (800°C–950°C) are all events which increase porosity.

The use of slate as a raw material has great potential due to its physical and chemical properties, them being similar to natural clays. Its powder may be used: in extrusion processes to produce tiles and bricks; as a filler in various ceramic processing; as a concrete aggregate; and, if heat treated, may be employed as a light aggregate, in the production of artificial stone materials for many applications.

ACKNOWLEDGEMENTS

The authors express their gratitude to the Brazilian funding agency (CAPES) for financial support. Kind donation of the slate powder by Micapel Slate Company is greatly appreciated.

REFERENCES

- [1] ABIROCHAS - Associação Brasileira da Indústria de Rochas Ornamentais. Brasília, DF. Disponível em: https://abirochas.com.br/wp-content/uploads/2022/01/Informe_05_2018_Setor_de_Rochas_Ornamentais_c.pdf. Accessed: 07 Jan. 2022.
- [2] OTI, J. E.; KINUTHIA, J. M.; BAI, J. Unfired clay masonry bricks incorporating slate waste. *W. Res. Management, Leeds*, v. 163, p. 17-27, Fev. 2010. DOI10.1680/warm.2010.163.1.17. Available in <https://doi.org/10.1680/warm.2010.163.1.17>
- [3] FRIAS, M. VIGIL-DE-LA-VILLA, R. GARCIA, R. SOTO, I. MEDINA, C. SANCHEZ-DE-ROJAS, M.I. Scientific and technical aspects of blended cement matrices containing activated slate wastes. *Cem Concr Compos.* v. 48, p. 19-25. Apr. 2014. DOI10.1016/j.cemconcomp.2014.01.002. Available in: <https://doi.org/10.1016/j.cemconcomp.2014.01.002>.
- [4] PALHARES, L. B., DOS SANTOS, C.G. AND HUNTER, T.N. Study of citric acid dispersant in the settling behavior of slate powder suspensions. *Int J Miner Process, Amsterdam*, v. 150, p. 39-46, May 2016. DOI. doi.org/10.1016/j.minpro.2016.03.005. Available in: <https://doi.org/10.1016/j.minpro.2016.03.005>
- [5] PALHARES, L.B., CARDOSO, A. V. Experiments with slip casting of fine ceramics and v-SiO₂. In: Gazzinelli, R. Moreira, R. L., Rodrigues, W. N. (org.). *Proceedings of Second International Conference on Physics and Industrial Development – Bridging the Gap*. Singapore: World Scientific, 1996. v. 1. p. 332-337.
- [6] CATARINO, L., SOUSA, J., MARTINS, I. M., VIEIRA, M. T., OLIVEIRA, M. M. Ceramic Products Obtained from Rock Wastes. *J. Mat. Proc. Tech. Amsterdam*, v. 143-144, p. 843-845, c1990, 2003. DOI10.1016/S0924-0136(03)00341-8. Available in: [https://doi.org/10.1016/S0924-0136\(03\)00341-8](https://doi.org/10.1016/S0924-0136(03)00341-8).

- [7] CAMBRONERO, L.E.F. RUIZ-ROMAN, J.M. RUIZ-PIETRO, J.M. Obtención de espumas a partir de residuos de pizarra. *Bol. de La Soc. Esp. Cer. y Vid. Madrid*, v. 44 (6), p. 368-372. DOI10.3989/cyv.2005y44.i6.330. Available in: <https://doi.org/10.3989/cyv.2005y44.i6.330>.
- [8] SILVA, M. E. M. C. PERES, A. E. C. Thermal expansion of slate wastes. *Miner Eng. New York*, v.19, p. 518-520, 2006. DOI10.1016/j.mineng.2005.10.008. Available in: <https://doi.org/10.1016/j.mineng.2005.10.008>.
- [9] SNELSON, D. G. OTI, J. E. KINUTHIA, J. M. BAI, J. Applications of slate waste material in the UK. *W. Rec. Management. Leeds*, v. 163, p. 19-15, 2010. DOI10.1680/warm.2010.163.1.9. Available in: <https://doi.org/10.1680/warm.2010.163.1.9>
- [10] ZHEN, L. et.al. Manufacturing of Ultra-light Ceramsite from Slate Wastes in Shangri-la, China. *J. K. Cer. Society. Seul*, v. 55, n.1, pp. 36-43, 2018. DOI10.4191/kcers.2018.55.1.02. Available in: <https://doi.org/10.4191/kcers.2018.55.1.02>.
- [11] CIESZKO, M., KEMPINSKI, M., CZERWINSKI, T. Limit models of pore space structure of porous materials for the determination of limit pore size distributions based on mercury intrusion data. *Transp. Porous Media, Springer*, v. 127, p. 433-458, 2019.
- DOI:10.1016/j.juogr.2016.02.002. Available in: <https://link.springer.com/article/10.1007/s11242-018-1200-5>.
- [12] ZHANG, L. et al. Effect of shearing actions on the rheological properties and mesostructures of CMC, PVP and CMC + PVP aqueous solutions as simple water-based drilling fluids for gas hydrate drilling. *J. Unconv. Oil Gas Resour, Elsevier*, v. 14, p. 86–98, 2016. DOI10.1016/j.juogr.2016.02.002. Available in: <https://doi.org/10.1016/j.juogr.2016.02.002>.
- [13] LARSON, A. C.; VON DREELE, R. B. General structure analysis system (GSAS). Los Alamos National Laboratory, Los Alamos, EUA, Copyright, 1985-2000, The Regents of the University of California, 2001.
- [14] CAMPOS, M. VELASCO, F. MARTINEZ, M. A. TORRALBA, J. M. Recovered slate waste as raw material for manufacturing sintered structural tiles. *J. Eur. Cer. Soc. Oxford-UK*, v. 24, p. 811-819, 2004. DOI10.1016/S0955-2219(03)00325-X. Available in: [https://doi.org/10.1016/S0955-2219\(03\)00325-X](https://doi.org/10.1016/S0955-2219(03)00325-X).
- [15] CHIODI FILHO, C. RODRIGUES, E. P. ARTUR, A.C. Ardósias de Minas Gerais, Brasil: Características Geológicas, Petrográficas e Químicas. *Geociências. São Paulo*, v. 22, n.2, p. 119-127., 2004. Available in: https://www.researchgate.net/publication/237351262_Ardosias_de_Minas_Gerais_Brasil_caracteristicas_geologicas_petrograficas_e_quimicas. Accessed on 25 Jan. 2018.
- [16] HILL, R.J., TSAMBOURAKIS, G., MADESEN, I.C. Improved petrological modal analysis from X-ray powder diffraction data by use of the Rietveld method. I. Selected igneous, volcanic, and metamorphic rocks. *J. of Petrology. Oxford-UK*, v.35, p. 867–900, 1993. DOI10.1093/petrology/34.5.867. Available in: <https://doi.org/10.1093/petrology/34.5.867>
- [17] MUMME, W.G., TSAMBOURAKIS, G., MADSEN, I.C., HILL, R.J. Improved petrological modal analysis from X-ray powder diffraction data by the use of the Rietveld method. II. Selected sedimentary rocks. *J. Sediment. Research. Tulsa*, v. 66, p.132–138, 1996. DOI10.1306/D42682D4-2B26-11D7-8648000102C1865D. Available in: <https://doi.org/10.1306/D42682D4-2B26-11D7-8648000102C1865D>

- [18] WEIDLER, P.G., LUSTER, J., SCHNEIDER, J., STICHER, H., GEHRING, A.U. The Rietveld method was applied to the quantitative mineralogical and chemical analysis of a ferritic soil. *Eur J Soil Sci. Oxford-UK*, v. 49, p. 95–105, 1998. DOI10.1046/j.1365-2389.1998.00138.x. Available in: <https://doi.org/10.1046/j.1365-2389.1998.00138.x>
- [19] GUGGENHEIM, S.; CHANG, Y., VAN-GROOS, A.F.K. Muscovite dehydroxylation: High-temperature studies. *American Mineralogist. Chantilly*, v. 72, p. 537- 550, 1987. Available in: https://rruff.geo.arizona.edu/doclib/am/vol72/AM72_537.pdf
- [20] HAZEN, R.M. Temperature, pressure, and composition: structurally analogous variables. *Phys Chem Miner. Berlin*, v. 1, p. 83-94, 1997. DOI10.1007/BF00307981. Available in: <https://doi.org/10.1007/BF00307981>.
- [21] SHU, Z. GARCIA-TEN, J. MORNFORT, E. AMOROS, J. L. ZHOU, J. WANG. Y. X. Cleaner production of porcelain tile powders - Fired compact properties. *Ceram Int. Oxford-UK*, v. 38, p. 1479-1487, 2012. DOI10.1016/j.ceramint.2011.09.031. Available in: <https://doi.org/10.1016/j.ceramint.2011.09.031>
- [22] SÁNCHEZ-SOTO, P. J. RUIZ-CONDE, A. BONO, R. RAIGÓN, M. GARZÓN, E. Thermal Evolution of a Slate. *J. Ther. Anal. Cal. Springer*, v. 90, p. 133–141, 2007. DOI10.1007/s10973-007-7751-2. Available in: <https://doi.org/10.1007/s10973-007-7751-2>.
- [23] MOURA, A. C., GRADE, J. As argilas do jazigo de Aguada de Cima: síntese dos resultados do seu estudo tecnológico aplicada à exploração. *Boletim de Minas*, 1977. Available in: <https://repositorio.ineg.pt/bitstream/10400.9/2427/1/34246.pdf>
- [24] COSTA, J. C.; ALMEIDA, T.; GOMES, C. S. F. Ardósia piro-expandida em arte escultórica. *Cerâmica. São Paulo*, v. 59, n. 349, p. 134-140, mar. 2013. DOI: 10.1590/S0366-69132013000100015. Available in: <https://doi.org/10.1590/S0366-69132013000100015>
- [25] PALHARES, L. B., DOS SANTOS, C. G., OLIVEIRA, V. A., FORTULAN, C. A., BINDA, F. F. Friction elements based on phenolic resin and slate powder. *J Mater Res Technol. Elsevier*, v. 9, n. 3, p. 3378-3383, 2020. DOI 10.1016/j.jmrt.2020.01.032. Available in: <https://doi.org/10.1016/j.jmrt.2020.01.032>
- [26] PALHARES, L.B., MANSUR, H.S. Production and characterization of ceramic pieces obtained by slip casting using powder wastes. *J Mater Process Techno. Amsterdam*, v.145, p.14-20, 2004. DOI10.1016/S0924-0136(03)00857-4. Available in: [https://doi.org/10.1016/S0924-0136\(03\)00857-4](https://doi.org/10.1016/S0924-0136(03)00857-4)

Sample number suspension	Green bulk density (g/cm ³) ± 0,1	Density after heat treatment (g/cm ³) ± 0,1	Volume reduction (%) (±1)	Green porosity (%) ± 0,1	Porosity after heat treatment (%) ± 0,1
1	2,1	1,9	17	56,9	46,9
2	2,4	2,2	19	56,5	45,7
3	2,5	2,4	19	55,4	43,5
4	2,7	2,6	23	59,6	44,6
5	2,5	2,4	23	63,4	45,4
6	2,4	2,2	22	64,7	41,1
7	3,5	2,7	24	50,5	39,8
8	3,4	2,6	25	50,9	43,4
9	3,1	2,4	26	52,9	46,5

Table 1: Green porosity/density of pieces and porosity/density after heat treatment,

Temp. (°C)	Specific surface BET (m ² /g)	Total Vol. of Pores (cm ³ /g)
100	12,26	0,0378
500	12,78	0,0365
700	9,99	0,0353
1000	4,76	0,0059
1100	4,22	0,0054

Table 2: Porosity and surface area of pieces after burning.

INTEGRATING E-LEARNING IN METAVERSE FOR SUSTAINABLE DEVELOPMENT OF HIGHER EDUCATION AND TRAINING

Acceptance date: 02/05/2024

Nguyen Duc Son

INTRODUCTION

ABSTRACT: Today, the development of information technology in the context of the industrial revolution 4.0 has changed the face of education rapidly and raised many new problems in this context. Along with that, the process of globalization has also given birth many non-traditional education methods. These types of education have transcended space, time, and types of boundaries. The article mentions the role and importance of metaverse in the global trend of higher education development through e-learning in the process of implementing cross-border education in universities all over the world. The article uses an interdisciplinary approach: education, science, and technology... to build a metaversity model in metaverse to develop training at universities in a sustainable way.

KEYWORDS: metaverse, metaversity, e-learning, borderless education.

Entering the 21st century, in the context of the industrial revolution 4.0, higher education has been applying information and communication technology to serve higher education. This is reflected in the digital transformation taking place in training institutions around the world. According to Susan Grajek and Betsy Reinitz [13], transfer process at universities around the world by 2020 indicates that 13% of colleges and universities are engaged in digital transformation, 32% are developing a digital transformation strategy and 38% of other higher education institutions are exploring digital transformation, only 17% of educational institutions do not have time to enter the process.

Along with that, the process of globalization has given birth to many non-traditional educational methods. New generations demand different delivery methods and curricular content. Flexibility and personalized offerings have become a common denominator in all sectors [11].

These types of education have transcended space, time, and types of boundaries. Many non-traditional educational models, such as virtual education..., were born, have been making it possible for new education providers to carry out educational work more smoothly than ever before. The emergence of the market for higher education services in the globalization trend is increasing [4]. Many university programs cross borders from universities through the internet and other means of distance education to learners worldwide. One of the new trends is distance education through “virtual universities” that can form and develop. A form of transition from an real university to a Metaverse university is the Hybrid university (Augmentation model – replicates everything and enables access anytime and form anywhere – using IT to virtualize the real environment as a means of broadening access [5]). IT has become a driving force in the formation of a global academic environment, and it also contributes to the connection, dissemination, and exchange of all achievements between universities, research institutes, production facilities and corporate groups around the world. There are many types of universities that apply information technology in training. However, main form of deployment is via the internet with e-learning. Currently, some popular forms of training by e-learning are: Technology - Based Training; Computer - Based Training; Web-Based Training; Online Learning/Training; Distance Learning. Nowadays, training model in the Metaverse - Metaversity environment has been formed a in the world.

DEFINITION

Metaverse

Neal Stephenson coined the term “metaverse” for the first time in his popular novel “Snow Crash” in 1992; and then Facebook rebranded as Meta and declared the metaverse to be Silicon Valley’s “next big thing” in 2021 [1].

The Metaverse is the post-reality universe, a perpetual and persistent multiuser environment merging physical reality with digital virtuality. It is based on the convergence of technologies that enable multisensory interactions with virtual environments, digital objects and people such as virtual reality (VR) and augmented reality (AR). Hence, the Metaverse is an interconnected web of social, networked immersive environments in persistent multiuser platforms. It enables seamless embodied user communication in real-time and dynamic interactions with digital artifacts. Its first iteration was a web of virtual worlds where avatars were able to teleport among them. The contemporary iteration of the Metaverse features social, immersive VR platforms compatible with massive multiplayer online video games, open game worlds and AR collaborative spaces [12].

Metaversity

A university inside the Metaverse [4]. It is a concept based on combining Metaverse and University. It is a Metaverse community-based education platform focused on empowering individuals with the skills and knowledge needed to teach and learn, as well as activities related to education and training. In addition, metaversity also helps training institutions and educators... generate income on the web3 in the Metaverse environment. The application of Metaverse in training implementation has been forming a “market” for cross-border education and a sustainable creative industry. Multimedia and interactive display in Metaversity is a new display method that gives learners a variety of experiences, excitement, and fun besides receiving one-way information. They can actively interact with each other, collaborate, and expand to learn more information and knowledge in all relevant fields in the metaverse [1].

The Deputy Minister of Information and Communications affirmed during the conference “The future of the internet”, over the past 20 years, Vietnam’s internet has developed strongly with a usage rate of 70.3%, becoming an essential need, and the foundation for the development of the digital economy and digital society. This is a great potential when digital transformation in higher education and virtual university application in Metaversity. If metaverse is applied in Vietnamese education, it will be a huge change, bringing practical benefits to learners, lecturers, and administrators, helping to access necessary information for managing and teaching and learning anywhere, anytime with good experiences in metaversity. The university will be better managed, more transparent, more economical and the quality of education will be improved. For examples: Greenwich Vietnam, also recently launched a new campus on Metavert (<https://meta.horizonland.app/>) [4]. It was only integrated into Metavert at first for enrollment and communication purposes. However, this has made a worthwhile contribution to increasing its reputation with the Greenwich Vietnam into community and give learners a good experience in Metavert’s ecosystem. The implementation of integrated teaching and learning on metaverse will be expanded and create a large educational ecosystem of Metaversity. With a virtual classroom supported by applications in Metaverse, participating learners can conduct learning and research at their own pace with mentor in the metaverse space; or even there is no mentor at all, simply learners participate in metaversity to experience, interact and create new content... There are virtual classrooms that contain a variety of ready-made learning materials that students can use. Students can follow up without the help of the instructor/ mentor. E-lecturer in this virtual classroom model replaces the lecturer to help learners based on pre-programmed situations and AI learned during e-learning operation.

Learners can have fun and experience with excitement in class instead of just passively studying in physics class. Integrating the interactive display of course content into the Metaverse environment is a new way of applying technology that changes the way

a classroom is run. There are many ways to participate in learning on Metaverse. It can be combined with a traditional classroom at a training facility with the metaverse. It can be combined with a traditional classroom at a training facility with the metaverse. Learners have the feeling that they are really in the classroom with the best experience for learning and developing the necessary skills. It provides the ability to visualize complex phenomena and gather information in the clearest and most complete way. In the metaversity environment, the learner themselves who will decide how and with whom to study... However, to maintain the quality of metaversity, it is necessary to apply the same process management and quality management philosophies to ensure a good training system, a good trainer system and a good digital content system. Metaversity creates an open higher education system with open input, open training, open assessment from many sides, and many perspectives.

METAVERSITY MODEL

Metaversity is a digitally built university using VR in the metaverse; a digital university campus is both in sync with and out of sync with the real world. Live Classes were taught by a qualified lecturer. And his lecture can be recorded and deployed to the content library in Metaversity for students to visit and experience for themselves later. Metaversity facilities make physical space “flat” (geographically), meaning that learners and teachers will interact in a virtual classroom environment in metaversity, even though they may be far apart. Smart devices are installed in the classroom to digitize the physical version of the classroom and exist in the Metaverse space as an extension and enhancement of the learner’s experience [3]. In the near future, Metaverse as a large society, combined with many technology businesses, also creates conditions for students to participate in virtual reality experiences and have the opportunity to access high technology. On the basis of this research, the paper proposes the following Metaversity model:

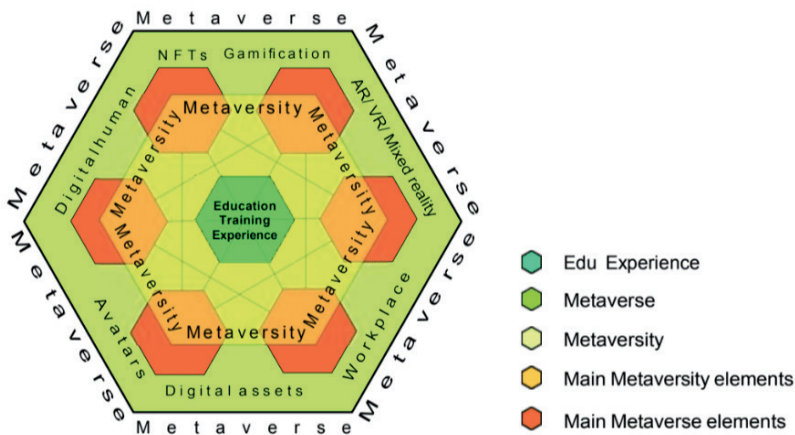


Fig. 1. Metaversity model

Metaversity is the result of integrating an entire university into Metaverse: Human (lecturers, administrators, students...); curriculums and teaching, learning materials; teaching methods; assets, facilities... All elements in the real world are digitized and operated in the Metaversity environment to provide the best teaching and learning experience (administrators, lecturers, students...)

Learning and teaching ecosystem

Metaversity (learning and teaching ecosystem in the metaverse) emerges and creates a social space for people to learn and share experiences in productive ways: Well-designed immersive environment with interactive way of visualization makes learning sessions focused and engaging with stronger and more memorable visuals. They can be created in the metaverse, both passive learning (the teacher conveys knowledge) and comprehension through reading (the learner read) is replaced by truly experiential learning. Learners can grab, manipulate, and walk around learning objects; they can be immersed in historical events; among many other opportunities.

In education and training, the learning-by-doing process is the best way to learn to accumulate knowledge and form skills, even if it is a large and complex project. As a result, learners are “embedded” in an immersive metaverse while they also use external peripherals to further enhance the learning experience. Overall, the metaverse is a very safe place for learners to “just be themselves” so that they actively learn at their own pace, making mistakes and making mistakes again, until the learning goal is accomplished. Moreover, learning from mistakes is also a good way to master skills. If learners do this in the real world, it will often be very expensive or impossible to do.

Metaverse also removes spatial barriers

No matter where learners are, they can enter the immersive world for any learning purpose. Usually, they are spatially sustainable. The learners and teachers from all over the world can interact and work as a team in the metaverse based on a conceptual model just like the real world (both in space and time).

The most compelling feature of the metaverse is that learners can interact with each other and with the instructor, no matter where they are located. Immersive Metaverse enables social and community learning experiences. Today, according to the International Telecommunication Union, 369 million young people do not have access to the Internet, resulting in exclusion, fewer educational resources and limited opportunities for children and young people to access the Internet. UNESCO also reports that 260 million children between the ages of 5 and 16 are out of school. Metaverse will be a connected ecosystem that brings opportunities and access to quality education for all. It acts as an educational

bridge in a very effective way. Universities need to work with customers, governments,... to bridge the digital divide in society, and promote educational programs like Connect To Learn, which help achieve the goals and Global Sustainable Development Goals at the same time. The transition from offline “classroom” to “Metaverse”, this is truly a journey to democratize education [1].

Due to the better interaction in the spatial and social structure of the metaverse, lecturers are also more likely to make requests to enhance work. A properly designed Metaversity environment will allow for the creation of entirely new ways of teaching and learning. Instructors can use role-playing techniques with avatars to present real-life situations. Learners can perform assignments easily because the 3D environment in the metaverse allows to simulate reality accurately [8]. From there, metaversity will build a skill database of learners (collecting different skills and storing them in a standardized skills database).

Learners can chat interactively and lively. In addition to video lectures, hosting live chats can be a good way to engage the learning community and make the learning process a lot more dynamic. A good learning management system will provide ways to interact with students in a virtual classroom. Interactions can be made via video, audio systems or can be live chat based on text input in the interactive screen. Thereby, it is possible to connect everyone in the virtual classroom together to enhance the student’s learning experience [9].

Incorporate instant feedback in Metaversity. Everyone feels encouraged to explore with instant feedback on how well they are doing. This can be done in virtual classrooms by taking advantage of one of the most popular features of a learning management system: automated assessment. These automated assessments will map to the e-lecturer’s expressions and actions so that students can see the results of their activities in the virtual classroom.

Metaverse helps deploy e-learning training anytime, anywhere, imparting knowledge on demand, providing quick feedback [9]. Learners can access the courses anywhere such as at the office, at home, at public Internet spots, 24 hours a day, 7 days a week. Join their virtual classroom on metaverse to meet the e-lecturer anytime they log-in to the virtual classroom.

Metaverse makes Virtual Classrooms more accessible to learners. Learners will no longer have to wait until class time to ask their lecturer questions: in a virtual classroom, they can be easily contacted to solve any problems while they are practicing [3]. Virtual classrooms with ready-made databases, role-playing-like organization...

Metaverse makes e-learning deployment more flexible. Students can choose from online instructor or self-interactive courses, adjust their learning pace according to their ability, and can enhance their knowledge through online libraries and supporting of e-lecturer [2].

Applying Metaverse

Applying Metaverse can focus on two main contents: in educational management and in teaching, learning, testing and evaluation: (1) In educational management, including digitizing management information, creating new system of large interconnected databases, application of AI technologies, blockchain, data analysis,...) to manage, operate, forecast, support decision making quickly and accurately; (2) In teaching, learning, testing and evaluation, including digital materials (e-textbooks, electronic lectures, e-learning lecture warehouses, multiple-choice question banks), digital libraries, laboratories,... virtual experience, deploy online training system, build virtual universities (cyber universities).

To build e-learning in the Metaverse environment, it will be necessary to convert traditional classrooms to digitize – visual/audio digital exercises for 24/7 learning and interaction. Learners and their mentors will automatically rely on the digital data to design a training program that is suitable for their ability and level. Lectures will be based primarily on supportive interactions and intensive teaching based on digitized fundamentals. Metaverse supports content innovation, teaching and learning methods, testing, and evaluation. Support effective implementation of synchronous solutions (including digital data e-learning lectures, electronic lesson design software, simulation software and teaching software). IoT, big data, artificial intelligence and machine learning AV/VR, security, blockchain, chatbots, Increased Accessibility... build and form a unified training ecosystem to connect hardware with software into smart, energy-efficient products and easily expand the system and Metaverse space. Grasping this trend of new digital technologies, universities can convert lectures into videos, play and learn (Gamification) to virtual reality (VR) and AR applications.

The simplest way is to use AR to add explanatory information about the images in the real space of the classroom, or simply on each image section of the reference book or a part of the classroom space with virtual classroom space in Metaverse. The Integrated Hybrid Classroom (combine online and offline at the same time) can even use AR to render 3D (digital versions) of models. Universities will not need to build large classrooms / lecture halls with a capacity of thousands of students. Instead, the university just builds presentations that can be created and saved in a virtual environment using digital technology or can be uploaded to Metaverse, setting up an online classroom directly in Metaverse... Learners can easily enter the classroom, access the lecture content data, and can download each part to learn (based on compliance with copyright law).

A lecturer's workflow in Metaverse could be: (1) first creating original immersive content that can be hosted in metaversity; (2) then this content will be assigned to a blockchain such as NFT and ensure that the blockchain used by the NFT is the same as used by the metaverse; (3) publish content in metaversity, assign rights and avail of viewing, using, modification and possible resale of the content [1]. Metaverse allows content creators with blockchain technology to turn into assets (cryptocurrency). These digital assets can be

used in the real world through rendering devices or traded under NFT as is the case with cryptocurrencies.

Even learners become content creators and can leverage their “property”. A student might create a product as part of a project assignment. Once converted and become part of the blockchain, that “creative” product will allow students to monetize the creation of digital assets. Thereby, learners can use their metaverse to communicate, connect, play some games, exhibit important solutions, co-create business projects, etc. Metaverse has gradually improved in terms of platform, scale, security, and partnerships to achieve one result: a dramatically enhanced learning experience that improves learning outcomes and the teaching experience.

Disadvantages of e-learning on Metaverse

In addition to the outstanding potential of being applied in the future, e-learning on Metaverse also has some disadvantages. Some common problems such as: emotional and spatial issues that make an impression on learners; Direct interaction with learners is limited due to limitations of technology. Need to be connected to high-speed internet (5G) and connect to many network-connected devices to learn. If there is a problem with the equipment or the transmission network, learning will be interrupted; Haven’t created a lively space like a traditional classroom.

Besides, Metaverse also requires computing power, and needs a large human resource of engineers, designers, and administrators to keep Metaverse up and working. Metaverse will need a large-scale technology infrastructure, from computing power to compute, 3D visualization to content for financial and trading systems. Going forward, Metaverse is still a technology built by many organizations. In addition, it is necessary to develop policies related to learning materials such as intellectual property, copyright; related to the quality of teaching in the network environment such as network information security [10]; related to personal information protection, information security in the network environment; and regulations related to the conditions for organization of online teaching and learning, quality accreditation, legality, and recognition of learning results...

CONCLUSION

In short, the digital era has now created very favorable opportunities to improve training quality and develop sustainably. Metaverse and gamification is one of the new trends in the context of the industrial revolution 4.0, helping to enhance the learner’s experience while improving the quality of training. It helps us a lot in training management, in all stages of the teaching and learning process: from preparing lesson outlines, designing programs, lectures, implementing subjects, exchanging and interacting with people learning, grading and exhibition, communication activities... can all be integrated with

multimedia in metaverse. By integrating multimedia, technology in the teaching and learning process will enable rich and vivid content transmissions in real or virtual contexts. VR or AR can help to enhance the interpretation of complex ideas, explore human knowledge, increase interaction opportunities, provide user experiences... Vietnam is on the road of Industrialization, Modernization, deep international integration in all areas of life, including education and training... The research and deployment of e-learning applications in the metaverse environment will help Vietnamese education develop quickly and sustainably.

ACKNOWLEDGMENT

I would like to express my appreciation to Mr. Nguyen Nhut Tan, director of Greenwich Vietnam, for his support during the planning and development of this research work.

I would also like to thank the staff of the Horizon Land for help and sharing information about Metaverse.

REFERENCES

1. Anand R., Katarina N., Matilda L., Mischa D., "Metaverse education: from university to metaversity", viewed 10th August 2022, <<https://www.ericsson.com/en/blog/2022/8/metaverse-education-from-university-to-metaversity>>.
2. Bilyalova A., Salimova D., Zelenina T. "Digital Transformation in Education. In: Antipova T. (eds) Integrated Science in Digital Age", ICIS 2019, Lecture Notes in Networks and Systems, vol 78. Springer, Cham. https://doi.org/10.1007/978-3-030-22493-6_24, 2020.
3. C. Suárez-Guerrero, C. Lloret-Catalá, S. Mengual-Andrés, Teachers' Perceptions of the Digital Transformation of the Classroom through the Use of Tablets: A Study in Spain, *Comunicar, Media Education Research Journal*, Volume 24, Issue 2. DOI: 10.3916/C49-2016-08, 2016.
4. Greenwich Vietnam in Metaverse, 2022, <https://meta.horizonland.app/>
5. Jay Liebowitz, *Digital Transformation for the University of the Future*, Digital Transformation: Accelerating Organizational Intelligence. 2023, World Scientific Publishing Co. Pte.Ltd.
6. Martin Carnoy. *Globalization, educational trends and the open society*. OSI Education Conference 2005: "Education and Open Society: A Critical Look at New Perspectives and Demands". Stanford University, School of Education, 2005.
7. Mystakidis, Stylianos. "Metaverse Encyclopedia", 2. 486-497. 10.3390/encyclopedia2010031, 2022.
8. Nguyễn Đức Sơn, "Nghệ thuật thiết kế tương tác & giao diện người dùng", Nxb Mỹ thuật, ISBN: 978 604 78 8549 7, 2018.
9. Nguyễn Đức Sơn, "Ứng dụng thiết kế web 3D VR nhằm tăng cường trải nghiệm người dùng", Hội thảo quốc tế về sáng tác nghệ thuật và thiết kế (IADW 2019), ISBN 978 604 68 5469 2, pp. 132 – 138, 2019.

10. Nehla Ghouaiel, Samir Garbaya, Jean-Marc Cieutat, Jean-Pierre Jessel, "Mobile Augmented Reality in Museums: Towards Enhancing Visitor's Learning Experience", *The International Journal of Virtual Reality*, 2016, 17(01): pp. 21-31.
11. Rodríguez-Abitia, G.; Bribiesca-Correa, G. Assessing Digital Transformation in Universities. *Future Internet* 2021, 13, 52. [https:// doi.org/10.3390/fi13020052](https://doi.org/10.3390/fi13020052).
12. Roger James Hamilton, "What is a Metaversity? Genius Group is changing the face of Education with Tech", LDN Staffer, viewed 15th August 2022, <<https://www.londondaily.news/what-is-a-metaversity- genius-group-is-changing-the-face-of-education-with-tech/>>.
13. Susan Grajek, Betsy Reinitz, "A Digital Transformation Pathway for Universities", 2023 World Scientific Publishing Company https://doi.org/10.1142/9789811254154_0001.

THERMAL PERFORMANCE OF A JACKETED MULTIPHASE OXYGEN REACTORS IN THE COPPER CHLORINE CYCLE FOR HYDROGEN PRODUCTION

Submission date: 19/03/2024

Acceptance date: 02/05/2024

Mohammed Wassef Abdulrahman
Rochester Institute of Technology

ABSTRACT: In this work, the heat transfer analysis of the three-phase oxygen reactor with a spiral baffled jacketed reactor are performed. The required number of oxygen reactors is analysed to provide enough heat input for different hydrogen production rates. Two types of fluids, which are helium gas and molten CuCl, are investigated to transfer heat from the jacket side to the process side of the oxygen reactor. In the analysis, the Cu-Cl cycle is assumed to be driven by a nuclear reactor where two types of nuclear reactors are examined as the heat source to the oxygen reactor. These types are the CANDU Super Critical Water Reactor (CANDU-SCWR) and High Temperature Gas Reactor (HTGR). In this work, it was found that the dominant contribution to the thermal resistance of the jacketed oxygen reactor system was from the reactor wall, where heat transfer occurred by conduction only. This contribution is about 80% of the total thermal resistance. It was also shown that a better heat transfer rate is required for SCWR than that for HTGR. Moreover, from

the study of the fluid types that can be used in the service side, it was recommended to use helium gas instead of molten CuCl as a heating fluid in the jacket. Finally, it was found that the size of the oxygen reactor must be specified from the heat balance studies rather than material balance.

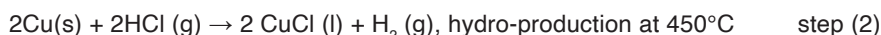
KEYWORDS: Cu-Cl cycle; hydrogen production; oxygen; heat transfer; Spiral Baffled Jacket

INTRODUCTION

Hydrogen as a clean energy carrier is frequently identified as a major solution to the environmental problem of greenhouse gases resulting from worldwide over dependence on fossil fuels. It is widely believed that hydrogen will be a significant contributing factor to sustainable energy supply in the future, since hydrogen reduces pollution of the atmosphere that contributes to climate change by reducing greenhouse gas emissions. Despite the exponentially growing need for hydrogen, the key challenge facing the hydrogen economy is the lack of sustainable production of hydrogen (without dependence on fossil

fuels) in large capacities at lower costs than existing technologies. Nuclear energy offers some potential as one of the sources for large scale of sustainable production of hydrogen.

Thermochemical cycles are the promising alternatives that could be linked with nuclear reactors to thermally decompose water into oxygen and hydrogen, through a series of intermediate reactions. Copper-chlorine (Cu-Cl) cycle is identified by the Argonne National Laboratories (ANL) as one of the most promising lower temperature cycles (Serban et. al., 2004). This cycle consists of four reactions, three thermal and one electrochemical. The four reaction steps of the Cu-Cl cycle are:



In the oxygen production step of the Cu-Cl cycle (step 4), an intermediate compound, solid copper oxychloride (Cu_2OCl_2), is decomposed into oxygen gas and molten cuprous chloride (CuCl). The solid feed of anhydrous solid Cu_2OCl_2 is supplied to the oxygen production reactor from the CuCl_2 hydrolysis reaction (step 3) that operates at a temperature range of 350–450°C. Gas species leaving the oxygen reactor include oxygen gas (which is evolved over a range a temperature range of 450 to 530°C) and potentially impurities of products from side reactions such as CuCl vapor, chlorine gas, HCl gas (trace amount) and H_2O vapour (trace amount). The substances exiting the reactor are molten CuCl and reactant particles entrained by the flow of molten CuCl. In the oxygen reactor, the decomposition of Cu_2OCl_2 to oxygen and molten CuCl is an endothermic reaction requiring a reaction heat of 129.2 kJ/mol and a temperature of 530°C, which is the highest temperature in the Cu-Cl cycle (Zamfirescu et. al., 2010). Thus, heat must be added to raise and maintain the temperature of the bulk inside the reactor.

Thermochemical properties of copper oxychloride have been examined by Ikeda and Kaye (2008) and more recently by Trevani et al. (2011). Since copper oxychloride is not commercially available, methods of synthesis were developed in these two studies. The method adopted by Ikeda and Kaye (2008) involved the use of stoichiometric amounts of CuO and CuCl_2 . Lewis et al. (2005), described briefly the experimental status of each of the Cu-Cl reactions. They investigated the evolution of oxygen when the $\text{Cu}_2\text{Cl}_2\text{O}$ was heated to 530°C. They further calculated that the total amount of oxygen recovered was after 25 minutes. Zamfirescu et al. (2010) examined the relevant thermo physical properties of compounds of copper that are used in thermochemical water splitting cycles. They

identified the available experimental data for properties of copper compounds relevant to the Cu–Cl cycle analysis and design (Cu_2OCl_2 , CuO , CuCl_2 and CuCl). They also developed new regression formulae to correlate the properties, which include: specific heat, enthalpy, entropy, Gibbs free energy, density, formation enthalpy and free energy. The properties were evaluated at 1 bar and a range of temperatures from ambient to 675–1000K, which are consistent with the operating conditions of the cycle. Marin (2012) provided new experimental and theoretical reference for the scale-up of a $\text{CuO}^*\text{CuCl}_2$ decomposition reactor with consideration of the impact on the yield of the thermochemical copper-chlorine cycle for the generation of hydrogen.

Abdulrahman et al. (2013a, 2016a, 2022a) have examined the scale-up feasibility of the oxygen reactor from the perspectives of the optimum size and number of oxygen reactors for different oxygen and hydrogen production rates. They specifically analysed the factors contributing to the oxygen reactor size. It was shown that the reactor size is significantly influenced by residence times, hydrogen production rate, mass and heat transfer. Abdulrahman (2016b, 2013b, 2019a, 2019b, 2022b) has investigated the scaleup analyses of the oxygen reactor from the perspective of indirect heat transfer using a half pipe and spiral baffled jacketed reactor and a helical tube inside the reactor (Abdulrahman, 2016c). He has concluded that the size of the reactor calculated from the perspective of heat balances is more than that calculated from the perspective of material balances. Different experiments have been performed to examine the hydrodynamics and direct contact heat transfer in the oxygen reactor (Abdulrahman, 2015, 2016d, 2016e, 2018, 2020a, 2019c). In the experiments, empirical equations have been formulated for the gas holdup and the direct contact heat transfer coefficient in the oxygen reactor. CFD simulations have been created to examine the hydrodynamics and heat transfer for the oxygen slurry bubble column reactor using two dimensional Eulerian-Eulerian approach (Abdulrahman, 2016f, 2016g, 2020b, 2020c, 2022c, 2022d, 2023a, 2023b, 2023c; Nassar, 2023).

In this work, the heat balance of the oxygen reactor in the Cu-Cl cycle is investigated analytically for different hydrogen production rates using a spiral baffled jacketed reactor. The thermal resistance of each section of the oxygen reactor system is investigated to examine the effect of each section on the heat balance. The heat balance of the oxygen reactor system is studied for Continuous Stirred Tank Reactor (CSTR) type that is heated by using a spiral baffled jacket. Two types of heat sources are studied which are Super Critical Water Reactor (SCWR) and High Temperature Gas Reactor (HTGR). Moreover, the type of the working fluid in the service side of the oxygen reactor system is examined for two types of fluids which are helium gas and CuCl molten salt, and a comparison between both fluids is performed.

THERMAL RESISTANCES

The continuous stirred-tank reactor (CSTR) is usually used for multiphase reactions that have fairly high reaction rates. Reactant streams are continuously fed into the vessel, and product streams are withdrawn. In CSTR, heating is achieved by a number of different mechanisms. The most common one involves the use of a jacket surrounding the vessel.

In a realistic continuous situation, where the reactor contents are at constant temperature, but with different service side inlet and outlet temperatures, the heat flow equation can be expressed by:

$$\dot{Q} = U A_s \Delta T_{lm} \quad (1)$$

where ΔT_{lm} is the log mean temperature difference between the bulk temperature of the reactor contents (cold temperature), T_c , and the temperature in the service side, T_H . Since the inside reactor temperature is assumed constant ($T_c=530^\circ\text{C}$), there is no effect of heat transfer configuration (parallel or counter flow) in the equation of ΔT_{lm} and can be written as:

$$\Delta T_{lm} = \frac{T_{H_{in}} - T_{H_{out}}}{\ln\left(\frac{T_{H_{in}} - T_c}{T_{H_{out}} - T_c}\right)} \quad (2)$$

The methodology of calculations depends on the comparison of thermal resistances of each section in the oxygen reactor with the calculated total thermal resistance of the reactor system (R_t). For a hydrogen production rate of 1 kg/day, the total amount of heat required in the oxygen reactor can be calculated as follows;

$$\dot{Q} = \Delta H_r \dot{\xi} + \dot{n} \int_{375}^{530} C_{p_{\text{Cu}_2\text{OCl}_2}} dT = 870 \text{ W} \quad (3)$$

where $\Delta H_r = 129.162 \text{ kJ/mol}$, $\dot{\xi} = 0.5 \text{ kmol/day}$, $\dot{n}_{\text{Cu}_2\text{OCl}_2} = 0.5 \text{ kmol/day}$, $C_{p_{\text{Cu}_2\text{OCl}_2}} = 134 \text{ J/mol.K}$ (Zamfirescu, 2010). The limits of the integral are from 375°C , which is the temperature of the fed solid, to 530°C , which is the temperature of the decomposition process. For a hydrogen production rate of 100 ton/day, $\dot{n}_{\text{Cu}_2\text{OCl}_2}$ is 50000 kmol/day and \dot{Q} will be 87 MW.

For a high temperature gas reactor (HTGR), the nuclear reactor exit temperature is about 1000°C . The inlet temperature of the heating fluid in the jacket (same as the exit temperature of the intermediate heat exchanger (IHE)) is about 900°C (Natesan, 2006). The exit temperature from the jacket is assumed to be 540°C (because the decomposition

temperature is 530°C). For a hydrogen production rate of 100 ton/day and number of reactors N , the total thermal resistance of the HTGR can be calculated as follows;

$$R_{HTGR} = \frac{1}{UA_s} = \frac{\Delta T_{lm}}{\dot{Q}} = 1.15 \times 10^{-6} N \text{ K/W} \quad (4)$$

For CANDU supercritical water reactor (CANDU-SCWR), where the nuclear reactor exit temperature is about 625°C (Chow & Khartabil, 2007; Duffey & Leung, 2010) and the inlet and outlet jacket temperatures are about 600°C and 540°C respectively, the total thermal resistance is $R_{SCWR} = 3.55 \times 10^{-7} N \text{ K/W}$ for a hydrogen production rate of 100 ton/day.

HEAT TRANSFER ANALYSIS

The resistance to the heat transfer is a composite of the resistances through the various sections indicated in Fig. 1. Using the classical film theory and heat conduction through composite layers, the total thermal resistance (R_t) can be expressed as;

$$R_t = R_P + R_{FP} = R_W = R_S = R_{FS}$$

$$= \frac{1}{h_P \pi D_P H_R} + \frac{f_P}{\pi D_P H_R} + \frac{\ln\left(\frac{D_S}{D_P}\right)}{2 \pi k_w H_R} + \frac{1}{h_S \pi D_S H_R} + \frac{f_S}{\pi D_S H_R} \quad (5)$$

The largest thermal resistance in Eq. (5) dominates the value of the overall heat transfer coefficient.

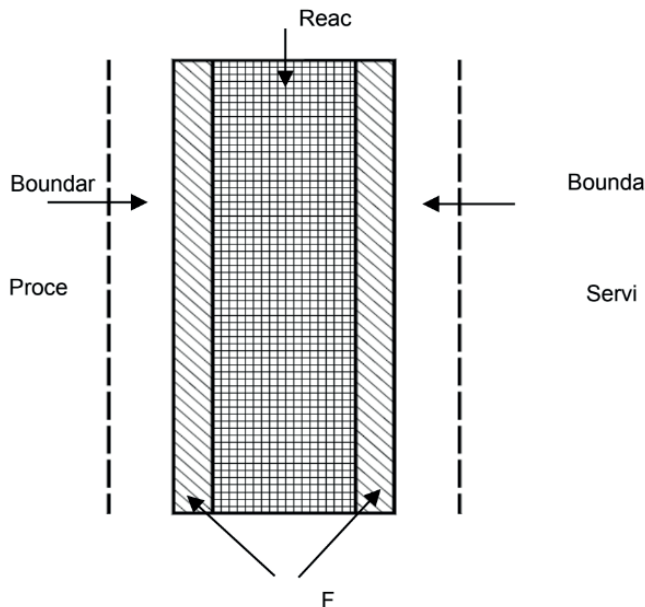


Fig. 1 Thermal resistances through the reactor wall sections.

Heat transfer through reactor wall

The stainless steels are the most frequently used corrosion resistant materials in the chemical industry. Types 321, 347 and 348 stainless steels are advantageous for high temperature service (such as in the oxygen reactor) because of their good mechanical properties. They continue to be employed for prolonged service in the 427°C to 816°C temperature range. The physical properties of Types 321, 347 and 348 are quite similar and, for all practical purposes, may be considered to be the same.

The ASME Code provides formulas that relate the wall thickness to the diameter, pressure, allowable stress, and weld efficiency. Since they are theoretically sound only for relatively thin shells, some restrictions are placed on their application. For cylindrical shell under internal pressure, the thickness in inches units is;

$$t = \frac{PR_R}{SE - 0.6P} + t_c \quad \text{conditions: } t \leq 0.25DR, \quad P \leq 0.385 SE \quad (6)$$

where t_c is the corrosion allowance in inches, R_R is the outside radius of the cylindrical shell in inches and S is the maximum allowable working stress in psi. P is the total pressure which is the sum of the static pressure and operating pressure of the oxygen reactor. The value of the joint efficiency, E , is between 0.6 and 1 (Abdulrahman, 2019b). In order to allow for possible surges in operation, it is customary to raise the maximum operating pressure by 10% or 0.69-1.7 bar over the maximum operation pressure, whichever is greater. The maximum operating pressure in turn may be taken as 1.7 bar greater than the normal (Couper et. al., 2005).

Heat transfer through spiral baffled jacket

The cross section of a spiral baffled jacket is shown in Fig. 2. The spacing between the jacket and reactor wall depends on the size of the reactor, however, it ranges from 50 mm for small reactors to 300 mm for larger reactors. In heat transfer applications, this jacket is considered a special spiral baffling case of a helical coil if certain factors are used for calculating outside film coefficients. The leakage around spiral baffles is considerable, amounting to 35–50% of the total mass flow rate. Due to the extensive leakage, the effective mass flow rate \dot{m}' in the jacket is usually taken as 60% of the actual flow rate \dot{m} to get a conservative film coefficient (Coker, 2001).

$$\dot{m}' \approx 0.6 \dot{m} = 0.6 \frac{\dot{Q}}{N C_p (T_{Hout} - T_{Hin})} \quad (7)$$

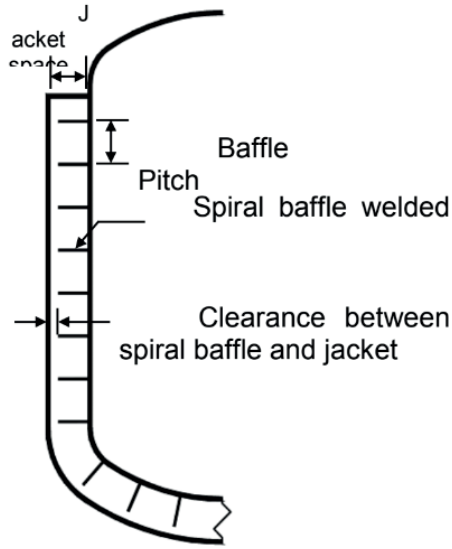


Fig. 2 Cross section of spiral baffled jacket.

where T_{in} and T_{out} are the jacket inlet and outlet temperature respectively. The velocity of the flow in the jacket can be calculated from the effective mass flow rate by;

$$u = \frac{\dot{m}'}{\rho A} \quad (8)$$

where A is the spiral baffled jacket cross sectional area and ρ is the density of the service side fluid (heating fluid). The pitch of the spiral baffled jacket can be calculated from;

$$p = \frac{A}{w} \quad (9)$$

where w is the width of the spiral baffled jacket. The number of coils of the spiral baffled jacket can be calculated from;

$$n = \frac{H_R}{p} \quad (10)$$

where H_R is the height of the reactor. The equivalent heat transfer diameter for the spiral baffled jacket is (Coker, 2001);

$$D_e = 4 w \quad (11)$$

At a given Reynolds number, heat transfer coefficients of coils, particularly with turbulent flow, are higher than those of long, straight pipes, due to friction. This also applies to flow through a spiral baffled jacket. The equation of heat transfer should be multiplied by a turbulent flow correction factor, involving the equivalent diameter and the diameter of the spiral coil. This correction factor is equal to $\{1 + 3.5 (D_e/D_c)\}$, where D_e is the equivalent heat transfer diameter for the spiral baffled jacket, which is calculated from (Coker, 2001): $D_e = 4w$, and D_c is defined as the centerline diameter of the jacket passage.

At $Re > 10,000$ the Sieder-Tate equation for straight pipe can be used to calculate the outside film coefficient (Coker, 2001);

$$Nu = 0.027 Re^{0.8} Pr^{0.33} \left(\frac{\mu_b}{\mu_w}\right)^{0.14} \left\{1 + 3.5 \left(\frac{D_e}{D_c}\right)\right\} \quad (12)$$

where D_c is defined as the centerline diameter of the jacket passage and is calculated as;

$$D_c = D_{ji} + \frac{D_{j0} - D_{ji}}{2} \quad (13)$$

where D_{ji} and D_{j0} are the inlet and outlet jacket diameter respectively. At $Re < 2,100$, the following equation can be used (Coker, 2001);

$$Nu = 1.86 Re^{0.33} Pr^{0.33} \left(\frac{\mu_b}{\mu_w}\right)^{0.14} \left(\frac{D_e}{L}\right)^{0.33} \quad (14)$$

where L is the length of the spiral baffled jacket. For $2,100 < Re < 10,000$, above equations can be used depending on the value of Re (Coker, 2001).

Process side heat transfer

Oxygen reactor is a multiphase reactor that contains solid particles (Cu_2OCl_2), molten salt ($CuCl$) and oxygen gas (O_2). In the study of indirect heat transfer, the presence of oxygen gas is neglected, because it is assumed that the oxygen gas will leave the reactor immediately after it is formed. The presence of solid particles will affect the viscosity of the molten salt. Since the density of the Cu_2OCl_2 solid (4080 kg/m^3) has a value near to that of the $CuCl$ molten salt (3692 kg/m^3), it is assumed that solid particles and molten salt are well mixed and form homogeneous slurry. This well mixed homogeneous slurry will lead to a more uniform temperature profile inside the oxygen reactor, that's why the temperature profile is assumed to be constant and equal to 530°C . Thermo physical properties are calculated for the slurry mixture at 530°C .

The dynamic viscosity of slurry can be described as relative to the viscosity of the liquid phase;

$$\mu_{SLR} = \mu_r \mu_L \quad (15)$$

where μ_r is the relative dynamic viscosity (dimensionless), μ_L is the dynamic viscosity of the liquid (CuCl molten salt). Depending on the size and concentration of the solid particles, several models exist to describe the relative viscosity as a function of volume fraction ϕ of solid particles.

$$\phi = \frac{V_S}{V_{SLR}} \quad (16)$$

where V_S and V_{SLR} are the volumes of solid particles and slurry respectively. In the case of extremely low concentrations of fine particles, Einstein's equation (Einstein, 1906) may be used;

$$\mu_r = 1 + 2.5 \phi \quad (17)$$

In the case of higher concentrations, a modified equation was proposed by Guth and Sima (1936), which considers interaction between the solid particles;

$$\mu_r = 1 + 2.5 \phi + 14.1 \phi^2 \quad (18)$$

Other thermo physical properties of the slurry mixture can be calculated from the volume percent of the solid and molten salt. For example, the average density of the slurry can be calculated as follows;

$$\rho_{SLR} = \rho_S \phi_S + \rho_L (1 - \phi_S) \quad (19)$$

where ρ_S and ρ_L are the densities of solid and liquid respectively. The average specific heat of the slurry is;

$$Cp_{SLR} = \frac{\rho_S Cp_S \phi_S + \rho_L Cp_L (1 - \phi_S)}{\rho_{SLR}} \quad (20)$$

where Cp_s and Cp_L are the specific heats of the solid and liquid respectively. A first order estimate of the effective thermal conductivity of a fluid filled porous media can be made by simply accounting for the volume fraction of each substance, giving the resulting relation based on the porosity and the thermal conductivity of each substance (Guth & Simba, 1936). Hence, the effective thermal conductivity of the slurry is calculated from;

$$k_{SLR} = k_s \phi_s + k_L (1 - \phi_s) \quad (21)$$

where k_s and k_L are the thermal conductivities of the solid and liquid respectively. For an agitated reactor, the inside film heat transfer coefficient (h_p) can be calculated from the following Nusselt number correlation (Coker, 2001);

$$Nu_D = C Re^a Pr^b \left(\frac{\mu}{\mu_w} \right)^c \quad (22)$$

where, C is constant, $Re = \text{Reynolds number} = \left(\frac{N_A D_A^2 \rho}{\mu_b} \right)$ and the agitator diameter $D_A = D_R/3$. The values of constant C and the indices a , b and c depend on the type of agitator, the use of baffles, and whether the transfer is to the vessel wall or to coils. An agitator is selected on the basis of material properties and the processing required. The heat transfer forms part of a process operation such as suspending or decomposing solid particles and dispersing the oxygen gas in the molten salt. Several methods for selecting an agitator are available (Kline, 1965; Himmelblau et. al., 2008). Penny (1970) showed one method based on liquid viscosity and vessel volume. According to the Penny's graph and the specifications of oxygen reactor contents and size, the type of the impeller that can be used is a propeller with 420 rpm. For baffled reactor, three blades propeller and transfer to reactor wall, the Nusselt number equation is (Coker, 2001);

$$Nu_D = 0.64 Re^{0.67} Pr^{0.33} \left(\frac{\mu_b}{\mu_w} \right)^{0.14} \quad (Re > 5000) \quad (23)$$

Fouling resistance

An important part of the specification for the oxygen reactor is the assignment of fouling effects. A recommended way to provide an allowance for fouling, is the use of individual fouling resistance values R_{fp} and R_{is} , for the two sides of the oxygen reactor as used in Eq. (5). R_{fp} is the fouling resistance that occurs on the internal surface of the reactor (process side) as a result of deposits that accumulate from the reactor contents. R_{fp} is the fouling resistance on the service side of the reactor (like jacket). For helium gas heating fluid, R_{fp} is expected to be negligible since there should be no build-up associated with clean dry helium. Values of the fouling resistances are specified which are intended to

reflect the values at the point in time just before the exchanger is to be cleaned. Fouling of heat exchange surfaces can cause a dramatic reduction in the performance of the reactor because of the relatively low thermal conductivity of the fouling material.

There are different approaches to provide an allowance for anticipated fouling in the design of oxygen reactor. In all, the result is to provide added heat transfer surface. This generally means that the reactor is oversized for clean operation and barely adequate for conditions just before it should be cleaned.

TYPE OF WORKING FLUID IN THE SERVICE SIDE OF OXYGEN REACTOR

Two types of fluids are highly recommended as working fluid in the oxygen reactor; CuCl molten salt and high-pressure helium gas (He). Helium gas is recommended amongst the other noble gases because of its chemical inertness and the relatively good transport properties (Rousseau & Van Ravenswaay, 2003; Wang et. al., 2002; Kikstra & Verkooijen, 2000).

There are substantial differences between molten salts and high-pressure helium that must be considered in selecting the working fluid as a heating medium in the oxygen reactor. These key differences are thermal performance, materials compatibility, and safety.

Thermal Performance

The thermo-physical properties for high-pressure helium and CuCl molten salt are summarized in Table 1.

Material	Molten Salt (CuCl) (Zamfirescu, 2010)	Helium (7.5 MPa)	Helium (2 MPa)
$T_{melting}$ ($^{\circ}C$)	430	-	-
$T_{boiling}$ ($^{\circ}C$)	1490	-	-
ρ (kg/m^3)	3692	3.5	0.939
C_p ($kJ/kg.^{\circ}C$)	0.66	5.2	5.2
ρC_p ($kJ/m^3.^{\circ}C$)	2450	18.2	4.883
k ($W/m.^{\circ}C$)	0.23	0.37	0.3687
$\mu \times 10^5$ ($pa.s$)	260	4.7	4.7
$\nu \times 10^6$ (m^2/s)	0.7	13.4	50
Pr	4.29	0.66	0.6624

Table 1 Comparison of thermo-physical properties of helium and CuCl molten salt at an average temperature of 750°C

From Table 1, it can be seen that the volumetric heat capacity, ρC_p , of molten salt is over two orders of magnitude greater than that of high-pressure helium. The much higher ρC_p of molten salts, compared to high-pressure helium, has a significant effect upon the relative heat transfer capability. In general, a molten salt loop uses piping of smaller diameters, and less pumping power than those required for high-pressure helium. These differences in pumping power and pipe size reduce the capital cost of the piping system, and allow the arrangement of process equipment to be optimized more easily since process heat can be delivered over larger distances easily. Also, heat transfer coefficients for molten salts are typically greater than those for helium.

Materials

Two primary aspects must be considered in selecting the high-temperature materials and heating fluid used for the oxygen reactor: corrosion and high-temperature mechanical properties (strength, creep, and fabric ability). Clean helium clearly does not have the potential to corrode loop materials, while, molten salts exhibit higher corrosion rates. The potential thermal performance advantages of molten salts suggest that the high-temperature corrosion testing with molten salts should be a priority for the oxygen reactor design.

Safety

The copper-chlorine process uses chemicals which are hazardous. The heat transfer fluid in the service side of oxygen reactor provides a stored energy source that can potentially be released rapidly, generating mechanical damage and potentially dispersing flammable or toxic chemicals. For helium gas, the stored energy comes from the high pressure of the gas, and the large volume of gas due to the large duct sizes required for transferring helium with reasonable pressure losses. For molten salts, the stored energy comes from the high temperature and high heat capacity of the liquid. This energy can be released if the molten salt mixes with a volatile liquid (e.g. water), through a well-studied phenomenon typically referred to as a “steam explosion.” Molten salts, due to their much lower pumping power and small piping size, permit greater physical separation between the nuclear reactor and the hydrogen production plant. This reduces or eliminates the need for berms or other structures to provide isolation between the reactor and hydrogen plant.

RESULTS AND DISCUSSION

Heat transfer calculations of the oxygen reactor system

The physical properties of the heating fluid in the service side of oxygen reactor are calculated at the mean temperature of the fluid, which is for a HTGR is 720°C and for SCWR is 570°C. Table 2 shows the physical properties of both helium and molten salt CuCl for both HTGR and SCWR.

Nuclear Reactor	Fluid	P (MPa)	ρ ($\frac{kg}{m^3}$)	μ $\times 10^{-5}$ ($\frac{kg}{m.s}$)	k ($\frac{W}{m.K}$)	Pr	Reference
HTGR (720°C)	Helium	1	0.48	4.6	0.36	0.66	(Petersen, 1970)
SCWR (570°C)	Helium	1	0.48	4.13	0.32	0.66	(Petersen, 1970)
HTGR (720°C)	CuCl	0.1	3692	146	0.19	5	(Zamfirescu, 2010)
SCWR (570°C)	CuCl	0.1	3692	188	0.2	6.11	(Zamfirescu, 2010)

Table 2 Physical properties of helium gas and CuCl molten salt for different mean temperatures

For a helium gas with a pressure of 1 MPa and a temperature range of 570-720°C, the compressibility factor range is 1.001426-1.009594 (Petersen, 1970). This factor varies from unity by less than 1% which means that helium gas can be regarded as an ideal gas. The equation of sound for gases is;

$$c = \sqrt{\gamma RT} \quad (24)$$

where γ is an adiabatic index ($\gamma_{He} = 1.6667$) and R is the gas constant ($R_{He} = 2077$ J/Kg. K). By using Eq. (24), the theoretical maximum speed of a helium gas (which is 1/3 of speed of sound) for a HTGR (T=720°C) is 618 m/s and for a SCWR (T=570°C) is equal to 570 m/s. In this work, to be more conservative for getting incompressible flow, the operating speed of the helium gas is considered to be 300 m/s in baffled jacket reactor for both HTGR and SCWR. The operating speed of the CuCl molten salt is assumed to be 3 m/s for baffled jacket. These values are within the range of molten salt nuclear reactors reported (Huntley & Silverman, 1976; Caire & Roure, 2007).

The physical properties of the slurry mixture inside the oxygen reactor (process side) are calculated from Eq. (15) to (21). Table 3 shows the physical properties of both the solid particles and the molten salt inside the oxygen reactor at a temperature of 530°C (Zamfirescu, 2010; Marin, 2012).

	$C_p \frac{J}{Kg.K}$	$k \frac{W}{m.K}$	$\rho \frac{Kg}{m^3}$
Solid Cu₂OCl₂	623.7	0.451	4080
Molten salt CuCl	650.8	0.2	3692

Table 3 Physical properties of Cu₂OCl₂ solid and CuCl molten salt at a temperature of 530°C

Heat transfer by jacketed reactor

To calculate the thermal resistance of the reactor wall, it is necessary to know the thickness of this wall. The thickness of the reactor wall (t) is calculated from Eq. (6). The pressure, P in Eq. (6) is the design pressure of the oxygen reactor which is taken here as 1.7 bar greater than the normal total pressure. The normal total pressure is the sum of the operating pressure (P_o) that is equal to 1 bar (14.5 psi) and the static pressure (P_s). Thus the design pressure is;

$$P = P_s + P_o + 1.7 \text{ (bar)} = \rho g H_R + P_o + 1.7 \text{ (bar)} \quad (25)$$

where ρ is the density of the slurry that is calculated from Eq. (19). The size of oxygen reactor has been estimated on the basis of the hydrogen production scale, mass balance, residence time, and aspect ratio, among others. The diameter range of 3-4 m and the aspect ratio of 2 were recommended for an industrial hydrogen production scale of over 100 tons/day (Abdulrahman, 2013a). In this work, the value of the reactor diameter is assumed to be 4 m and the height is 8 m.

The material of the reactor wall is assumed to be stainless steel 321 and the maximum allowable working stress (S) for this stainless steel is 3600 psi at $T=649^\circ\text{C}$ (Rozic, 1973). The value of the thermal conductivity (k_w) for stainless steel 321 in the temperature range of 20-500°C is 21.4 W/m.K (Wang et. al., 2002). For known corrosive conditions, the corrosion allowance (t_c) is 8.9 mm (0.35 in.) (Chenoweth, 1990). This value is used for the oxygen reactor because of the relative high corrosion susceptibility of CuCl molten salt. The joint efficiency E is taken as 0.8. By substituting the above values into Eq. (6), the thickness of the reactor with a diameter of 4 m and a height of 8 m will be, $t = 2.7 \text{ in} = 7 \text{ cm}$

In order to calculate the thermal resistance due to fouling in the oxygen reactor, the fouling factor must be known or estimated. According to Tubular Exchanger Manufacturers Association (TEMA), the fouling factor for molten heat transfer salts is equal to 0.000088 m² K/W (Chenoweth, 1990). In this work, to be more conservative, twice of this value, 0.000176 m² K/W, is used to be the fouling factor for molten salt CuCl.

To calculate the thermal resistance of the jacket side, it is assumed that the thickness of the jacket for spiral baffled jacket is $D_R/15$, where D_R is the reactor diameter. Table 4 shows the values of the numbers of oxygen reactors required for each section of the oxygen reactor

for different heating fluids and different nuclear reactors. Figure 3 shows a comparison of the number of reactors required between HTGR and SCWR. This comparison is for each section of the oxygen reactor system with a helium gas at a pressure of 1MPa. From Table 4 and Fig. 3, it can be seen that the maximum number of reactors required comes from the wall of the reactor. This is because of the large thickness and small conductivity of the wall material. The large diameter requires thick wall to provide enough mechanical stresses and the large height produces high static pressure inside the reactor, which in turn requires more thickness for the wall. It can be seen also that the number of oxygen reactors for SCWR are higher than that for HTGR by more than three times. This is because of the higher temperature difference between the service and process sides in the HTGR. This means that using HTGR is more efficient for producing heat to the oxygen reactor than SCWR. Figure 4 shows the total number of jacketed oxygen reactors with each nuclear reactor for both helium gas and CuCl molten salt. From this figure, it can be seen that there is no big differences between helium gas and molten CuCl in heating the jacketed oxygen reactor.

Fig. 5 shows the comparison of number of oxygen reactors versus the hydrogen production rate between material balance and heat balances for both HTGR and SCWR for a residence time of 0.5 hr and for helium gas service fluid. From Fig. 5, it can be seen that the numbers of reactors calculated from heat balance are 18 times higher than that calculated from material balance for HTGR and 57 times for SCWR. That means the design of oxygen reactor size is controlled mainly by the heat balance.

Nuclear Reactor Type	Fluid Type	P (MPa)	N_p	N_{FP}	N_w	N_{FS}	$N_{S-baffle}$	$N_{total-baffle}$
HTGR	He	1	1.4	1.5	27.8	0	3.4	35
	CuCl	0.1				1.5	1.4	34
SCWR	He	1	4.9	4.9	90	0	13	113
	CuCl	0.1				4.8	4.6	110

Table 4 Number of reactors of each section of the jacketed oxygen reactor system for different heating fluids and different nuclear reactors

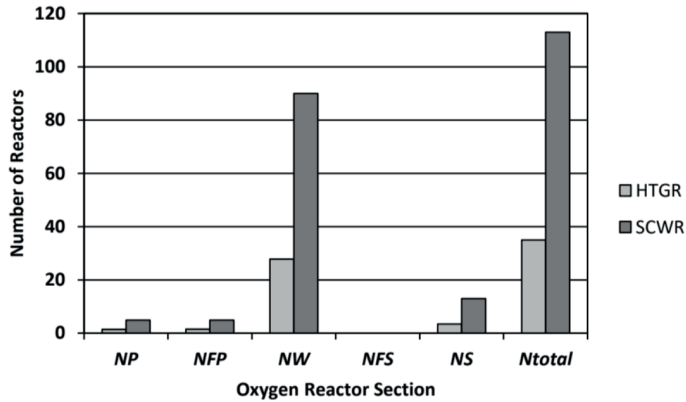


Fig. 3 Number of reactors for each section in oxygen reactor system heated by 1MPa helium gas for both HTGR and SCWR.

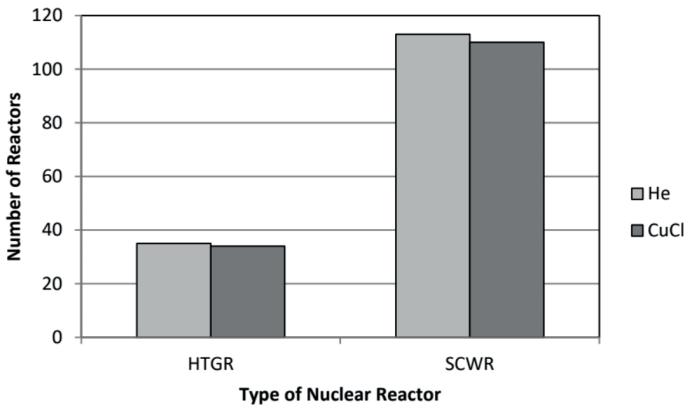


Fig. 4 Total number of oxygen reactors with each nuclear reactor for both 1MPa helium gas and CuCl molten salt.

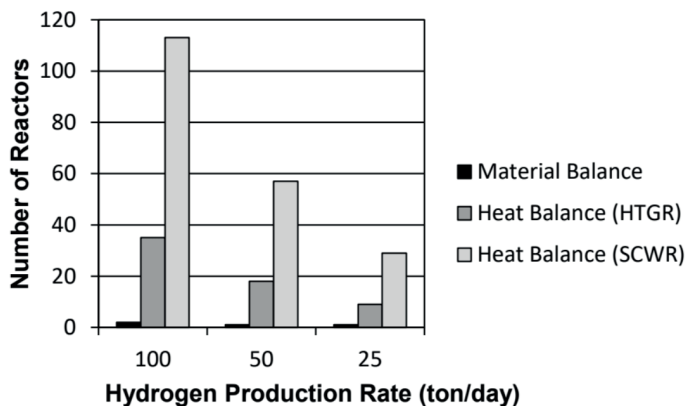


Fig. 5 Number of oxygen reactors calculated by material balance and heat balances of both HTGR and SCWR versus hydrogen production rate for a residence time of 0.5 hr.

CONCLUSIONS

In this work, it can be concluded that the dominant heat transfer thermal resistance of the jacketed oxygen reactor system, is from the reactor wall which contributes in about 80% of the total thermal resistance for both types of heat sources (SCWR and HTGR). The service side contributes in about 10% and the process side and fouling in about 4% for each. The high thermal resistance of the wall is due to the large thickness and small thermal conductivity of the reactor wall.

Heat transfer calculations showed that the total thermal resistance needed for SCWR is less than that for HTGR. That means a better heat transfer rate is required for SCWR than that for HTGR. Thus, HTGR is more efficient than SCWR in providing the required heat for the thermal decomposition process inside the oxygen reactor, because of the highest temperature difference between the service and process side in HTGR than in SCWR.

From the comparison study of the type of fluid in the service side, it is concluded that the thermal performance of the molten CuCl is better than that of helium gas which in turn is better than molten CuCl from the perspectives of material and safety aspects. By comparing the number of reactors for both fluids, it is shown that there is no significant difference between both fluids and in this case, it is recommended to use helium gas as a heating fluid in the service side of the oxygen reactor system.

From the comparison of the number of reactors obtained from material and heat balances, it is concluded that the size of the oxygen reactor is specified from the heat balance study rather than material balance.

REFERENCES

Abdulrahman, M. W. (2015). Experimental studies of direct contact heat transfer in a slurry bubble column at high gas temperature of a helium–water–alumina system. *Applied Thermal Engineering*, 91, 515-524.

Abdulrahman, M. W. (2016a). *Analysis of the thermal hydraulics of a multiphase oxygen production reactor in the Cu-Cl cycle*. University of Ontario Institute of Technology (Canada).

Abdulrahman, M. W. (2016b). Similitude for thermal scale-up of a multiphase thermolysis reactor in the cu-cl cycle of a hydrogen production. *World Academy of Science, Engineering and Technology, International Journal of Electrical, Computer, Energetic, Electronic and Communication Engineering*, 10(5), 567-573.

Abdulrahman, M. W. (2016c). Heat transfer analysis of a multiphase oxygen reactor heated by a helical tube in the cu-cl cycle of a hydrogen production. *World Academy of Science, Engineering and Technology, International Journal of Mechanical, Aerospace, Industrial, Mechatronic and Manufacturing Engineering*, 10(6), 1018-1023.

Abdulrahman, M. W. (2016d). Experimental studies of gas holdup in a slurry bubble column at high gas temperature of a helium– water– alumina system. *Chemical Engineering Research and Design*, 109, 486-494.

- Abdulrahman, M. W. (2016e). Experimental studies of the transition velocity in a slurry bubble column at high gas temperature of a helium–water–alumina system. *Experimental Thermal and Fluid Science*, 74, 404-410.
- Abdulrahman, M. W. (2016f). CFD simulations of direct contact volumetric heat transfer coefficient in a slurry bubble column at a high gas temperature of a helium–water–alumina system. *Applied thermal engineering*, 99, 224-234.
- Abdulrahman, M. W. (2016g). CFD Analysis of Temperature Distributions in a Slurry Bubble Column with Direct Contact Heat Transfer. In *Proceedings of the 3rd International Conference on Fluid Flow, Heat and Mass Transfer (FFHMT'16)*.
- Abdulrahman, M. W. (2018). *U.S. Patent No. 10,059,586*. Washington, DC: U.S. Patent and Trademark Office.
- Abdulrahman, M. W. (2019a). Heat transfer in a tubular reforming catalyst bed: Analytical modelling. In *proceedings of the 6th International Conference of Fluid Flow, Heat and Mass Transfer*.
- Abdulrahman, M. W. (2019b). Exact analytical solution for two-dimensional heat transfer equation through a packed bed reactor. In *Proceedings of the 7th World Congress on Mechanical, Chemical, and Material Engineering*.
- Abdulrahman, M. W. (2019c). Simulation of Materials Used in the Multiphase Oxygen Reactor of Hydrogen Production Cu-Cl Cycle. In *Proceedings of the 6 the International Conference of Fluid Flow, Heat and Mass Transfer (FFHMT'19)* (pp. 123-1).
- Abdulrahman, M. W. (2020a). *U.S. Patent No. 10,526,201*. Washington, DC: U.S. Patent and Trademark Office.
- Abdulrahman, M. W. (2020b). Effect of Solid Particles on Gas Holdup in a Slurry Bubble Column. In *Proceedings of the 6th World Congress on Mechanical, Chemical, and Material Engineering*.
- Abdulrahman, M. W. (2020c). CFD Simulations of Gas Holdup in a Bubble Column at High Gas Temperature of a Helium-Water System. In *Proceedings of the 7th World Congress on Mechanical, Chemical, and Material Engineering (MCM'20)* (pp. 169-1).
- Abdulrahman, M. W. (2022a). Review of the Thermal Hydraulics of Multi-Phase Oxygen Production Reactor in the Cu-Cl Cycle of Hydrogen Production. In *Proceedings of the 9th International Conference on Fluid Flow, Heat and Mass Transfer (FFHMT'22)*.
- Abdulrahman, M. W. (2022b). Heat Transfer Analysis of the Spiral Baffled Jacketed Multiphase Oxygen Reactor in the Hydrogen Production Cu-Cl Cycle. In *Proceedings of the 9th International Conference on Fluid Flow, Heat and Mass Transfer (FFHMT'22)*.
- Abdulrahman, M. W. (2022c). Temperature profiles of a direct contact heat transfer in a slurry bubble column. *Chemical Engineering Research and Design*, 182, 183-193.
- Abdulrahman, M. W., & Nassar, N. (2022d). Eulerian Approach to CFD Analysis of a Bubble Column Reactor–A. In *Proceedings of the 8th World Congress on Mechanical, Chemical, and Material Engineering (MCM'22)*.

- Abdulrahman, M. W., & Nassar, N. (2023a). A Three-dimensional cfd analyses for the gas holdup in a bubble column reactor. In *Proceedings of the 9th World Congress on Mechanical, Chemical, and Material Engineering (MCM'23)*.
- Abdulrahman, M. W., & Nassar, N. (2023b). Three dimensional cfd analyses for the effect of solid concentration on gas holdup in a slurry bubble column. In *Proceedings of the 9th World Congress on Mechanical, Chemical, and Material Engineering (MCM'23)*.
- Abdulrahman, M. W., & Nassar, N. (2023c). Effect of static liquid height on gas holdup of a bubble column reactor," In *Proceedings of the 9th World Congress on Mechanical, Chemical, and Material Engineering (MCM'23)*.
- Abdulrahman, M. W., Wang, Z., & Naterer, G. F. (2013a). Scale-up analysis of three-phase oxygen reactor in the Cu-Cl thermochemical cycle of hydrogen production. In *EIC Climate Change Technology Conference*.
- Abdulrahman, M. W., Wang, Z., Naterer, G. F., & Agelin-Chaab, M. (2013b). Thermohydraulics of a thermolysis reactor and heat exchangers in the Cu-Cl cycle of nuclear hydrogen production. In *Proceedings of the 5th World Hydrogen Technologies Convention*.
- Boomsma, K., & Poulikakos, D. (2001). On the effective thermal conductivity of a three-dimensionally structured fluid-saturated metal foam. *International journal of heat and mass transfer*, 44(4), 827-836.
- Caire, J. P., & Roure, A. (2007). Pre design of a molten salt thorium reactor loop.
- Chenoweth, J. M. (1990). Final report of the HTRI/TEMA joint committee to review the fouling section of the TEMA standards. *Heat Transfer Engineering*, 11(1), 73-107.
- Chow, C. K., & Khartabil, H. F. (2008). Conceptual fuel channel designs for CANDU-SCWR. *Nuclear Engineering and Technology*, 40(2), 139-146.
- Coker, A. K. (2001). *Modeling of chemical kinetics and reactor design*. Gulf Professional Publishing.
- Couper, J. R. (2005). *Chemical process equipment: selection and design*. Gulf professional publishing.
- Duffey, R. B., & Leung, L. (2010). Advanced cycle efficiency: generating 40% more power from the nuclear fuel.
- Einstein, A. (1906). A new determination of molecular dimensions. *Annln., Phys.*, 19, 289-306.
- Guth, E., & Simba, H. (1936). Viscosity of suspensions and solutions: III Viscosity of sphere suspensions. *Kolloid-Zeitschrift*, 74, 266-275.
- Himmelblau, D. M., Bisio, A., & Kabel, R. L. (2008). *Scaleup of chemical processes*. John Wiley & Sons.
- Huntley, W. R., & Silverman, M. D. (1976). *System design description of forced-convection molten-salt corrosion loops MSR-FCL-3 and MSR-FCL-4* (No. ORNL/TM--5540). Oak Ridge National Lab.
- Ikeda, B. M., & Kaye, M. H. (2008, August). Thermodynamic properties in the Cu-Cl-OH system. In *7th International conference on nuclear and radiochemistry, Budapest, Hungary*.

- Kikstra, J. F., & Verkooijen, A. H. M. (2000). Conceptual design for the energy conversion system of a nuclear gas turbine cogeneration plant. *Proceedings of the Institution of Mechanical Engineers, Part A: Journal of Power and Energy*, 214(5), 401-411.
- Kline, S. J. (1965). *Similitude and approximation theory*. New York, McGraw-Hill.
- Lewis, A., Masin, J. G. & Vilim, R. B. (2005). Development of the low temperature cu-cl thermochemical cycle. in *Proceedings of the International Congress on Advances in Nuclear Power Plants*, Argonne National Laboratory, Seoul, Korea.
- Marin, G. D. (2012). *Kinetics and Transport Phenomena in the Chemical Decomposition of Copper Oxychloride in the Thermochemical Copper Chloride Cycle*. University of Ontario Institute of Technology (Canada).
- Nassar, N. I. (2023). *A Three-Dimensional CFD Analyses for the Hydrodynamics of the Direct Contact Heat Transfer in the Oxygen Production Slurry Bubble Column Reactor of the Cu-Cl Cycle of Hydrogen Production*. Rochester Institute of Technology.
- Natesan, K., Moisseytsev, A., & Majumdar, S. (2009). Preliminary issues associated with the next generation nuclear plant intermediate heat exchanger design. *Journal of nuclear materials*, 392(2), 307-315.
- Penny, W. R. (1970). Guide to trouble free mixers. *Chem. Eng.*, vol. 77, no. 12, p. 171.
- Petersen, H. (1970). *The properties of helium: density, specific heats, viscosity, and thermal conductivity at pressures from 1 to 100 bar and from room temperature to about 1800 K*. Copenhagen: Jul. Gjellerup.
- Rousseau, P. G., & Van Ravenswaay, J. P. (2003, May). Thermal-fluid comparison of three-and single-shaft closed loop brayton cycle configurations for htgr power conversion. In *Proceedings of International Congress on Advances in Nuclear Power Plants (ICAPP'03)*.
- Rozic, E. J. (1973). *Elevated temperature properties as influenced by nitrogen additions to types 304 and 316 austenitic stainless steels*. ASTM International.
- Serban, M., Lewis, M. A., & Basco, J. K. (2004). *Kinetic study of the hydrogen and oxygen production reactions in the copper-chloride thermochemical cycle*. American Institute of Chemical Engineers.
- Trevani, L. (2011, May). The copper-chloride cycle: synthesis and characterization of copper oxychloride. In *Hydrogen and Fuel Cells International Conference and Exhibition*.
- Wang, C., Ballinger, R. G., Stahle, P. W., Demetri, E., & Koronowski, M. (2002). Design of a power conversion system for an indirect cycle, helium cooled pebble bed reactor system.
- Zamfirescu, C., Dincer, I., & Naterer, G. F. (2010). Thermophysical properties of copper compounds in copper–chlorine thermochemical water splitting cycles. *International Journal of Hydrogen Energy*, 35(10), 4839-4852.

CHAPTER 4

ADVANCES IN THERMAL HYDRAULICS OF OXYGEN PRODUCTION REACTORS IN THE COPPER-CHLORINE CYCLE FOR HYDROGEN PRODUCTION: A COMPREHENSIVE REVIEW

Submission date: 19/03/2024

Acceptance date: 02/05/2024

Mohammed Wassef Abdulrahman

Rochester Institute of Technology
Dubai / UAE

KEYWORDS: Hydrogen Production; Cu-Cl Cycle; Thermolysis; Oxygen Production; Scale up.

ABSTRACT: The thermochemical water splitting process using the copper-chlorine (Cu-Cl) cycle is an innovative method for generating hydrogen gas. This process involves a thermolysis reaction where molten salt, a solid reactant, and gaseous oxygen interact to produce oxygen gas. The primary aim of this work is to contribute to the development and enhancement of the thermochemical Cu-Cl cycle for hydrogen production. To achieve this goal, a comprehensive review of the multiphase oxygen generation reactor, which is a crucial component of the Cu-Cl cycle, is conducted. The review covers various aspects of the oxygen reactor, including; type and description of the Oxygen reactor, material features, variables affecting reactor's size, and scale-up evaluations. This work aims to provide a thorough understanding of the oxygen reactor in the Cu-Cl cycle, highlighting its significance in the thermochemical production of hydrogen and the key considerations for its optimization and scale-up.

INTRODUCTION

Hydrogen is increasingly recognized as a pivotal solution to the environmental challenges posed by greenhouse gas emissions, which are largely attributed to the global dependence on fossil fuels. It is widely regarded as a significant contributor to the future sustainable energy supply, as its utilization can substantially reduce atmospheric pollution and mitigate climate change by lowering greenhouse gas emissions (Forsberg, 2007). Given its versatile applications across various industries, the demand for hydrogen is projected to rise considerably in the forthcoming decade.

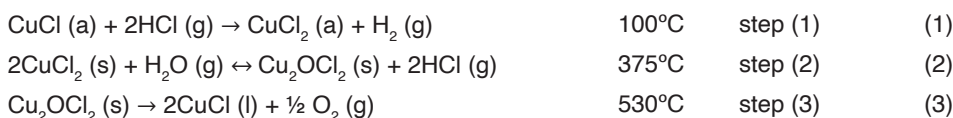
The majority of hydrogen production on a global scale currently relies on methods such as steam-methane reforming or partial oxidation of heavy hydrocarbons. While these processes are efficient, they generate substantial quantities of carbon

dioxide, contributing to greenhouse gas emissions. These conventional methods are facing increasing challenges due to escalating greenhouse gas emissions, reducing natural gas resources, and rising costs associated with carbon capture and storage.

In light of the exponential growth in demand for hydrogen, the primary challenge for the hydrogen economy is the sustainable generation of hydrogen on a large scale, without dependence on fossil fuels, and at costs lower than those of existing technologies. In this context, nuclear energy emerges as a potential source for large-scale, sustainable hydrogen production.

Thermochemical cycles represent a promising alternative that can be integrated with nuclear reactors to thermally decompose water into oxygen and hydrogen through a series of intermediate processes. These cycles facilitate the transfer of heat between different reactors, some of which are endothermic and others exothermic, via heat exchangers that either provide or recover heat from specific processes. The copper-chlorine (Cu-Cl) cycle, identified by Argonne National Laboratories (ANL) as one of the most promising low-temperature cycles, stands out in this regard (Lewis et. al 2003; Serban et. al., 2004). One of the most notable advantages of the Cu-Cl cycle is its lower temperature requirement compared to many other cycles, which enhances its efficiency and accessibility. Furthermore, the cycle can be conducted in a manner that necessitates minimal high-quality energy and solid exchanges, making it more environmentally and economically viable.

The integration of this cycle with nuclear energy offers a sustainable pathway for hydrogen generation, addressing the pressing need for clean energy solutions. As the world moves towards a more sustainable energy future, the development and optimization of thermochemical cycles like the Cu-Cl cycle, in conjunction with advancements in nuclear technology, hold great promise for meeting the growing demand for hydrogen while mitigating the environmental impact of energy production. This cycle comprises three reactions: two thermal and one electrochemical. The Cu-Cl cycle comprises three reactions, two thermal and one electrochemical:



where *a*, *s*, *l* and *g* denote to aqueous, solid, liquid and gas respectively.

In the oxygen generation stage (step 3), an intermediate chemical known as solid copper oxychloride (Cu_2OCl_2) undergoes decomposition, resulting in the formation of oxygen gas and molten cuprous chloride (CuCl). This stage is crucial for the overall efficiency of the Cu-Cl cycle. The oxygen generation reactor receives an input of anhydrous solid Cu_2OCl_2 from the preceding step in the cycle, which is the hydrolysis of CuCl_2 . This hydrolysis process operates at temperatures ranging from 350 to 450°C. Once inside the oxygen reactor, the solid Cu_2OCl_2 is subjected to higher temperatures, typically between 450 and 530°C, which triggers its decomposition into oxygen gas and molten CuCl .

However, the process is not without its challenges. The gaseous output from the oxygen reactor may include not only the desired oxygen gas but also potential contaminants from side reactions. These could include vaporized CuCl, chlorine gas, and trace amounts of hydrochloric acid (HCl) gas and water vapor (H₂O). These by-products need to be carefully managed to ensure the purity of the produced oxygen and the overall efficiency of the cycle.

Moreover, the substances exiting the reactor are primarily molten CuCl, but there might also be solid CuCl₂ present. This can occur due to the incomplete breakdown of CuCl₂ at temperatures below 750°C (Micco et. al., 2007). Additionally, reactant particles may be entrained in the flow of molten CuCl, further complicating the process.

Overall, the oxygen generation stage of the Cu-Cl cycle is a complex process that requires careful control and management to ensure its efficiency and effectiveness in contributing to the sustainable production of hydrogen.

OXYGEN REACTOR TYPE

Three phases comprise the oxygen reactor: the solid phase (copper oxychloride particles), the liquid phase (molten salt), and the leaving gaseous phase (oxygen). In chemical, petroleum, and biological processes, multiphase reactions such as gas/liquid/solid are often employed. The industry offers various different kinds of multiphase reactors, which may be grouped into two broad categories: fixed bed reactors and slurry phase reactors. Fixed bed or packed bed reactors have a stationary solid phase. Because the oxygen reactor's solid phase is continuous, it cannot be termed a fixed bed reactor (Abdulrahman, 2016a). Stirred tank reactors (STR) and slurry bubble column reactors are the most common continuous slurry phase reactors (SBCRs). The continuous stirred tank reactor (CSTR), which is often used for liquid-phase or multiphase processes with moderate reaction rates, is a mechanically agitated reactor in which small particles are suspended in the liquid phase by agitation. Continuous reaction streams are supplied into the vessel, while product streams are removed. In general, a continuous flow stirred tank reactor (CFSTR) implies that the fluid is properly mixed, ensuring that the reaction mixture's parameters (e.g., concentration, density, and temperature) remain uniform throughout the system. As a result, the conditions throughout the reactor are same, and the temperature at the reactor output is identical. The solid phase in the SBCR is composed of small particles suspended in the liquid phase as a result of gaseous bubbles supplied from the bottom, often through a sparger (Abdulrahman, 2016a; Li et. al., 2016).

Oxygen reactors may be classified as CFSTRs or SBCRs. The decision between these two kinds of reactors is determined by the heat transfer rate efficiency, the agitation efficiency, the ability to scale up, and other design requirements. The oxygen reactor's thermal design demands adequate agitation inside the reactor and a sufficiently high rate of heat transfer to the solid particles. Agitation may be accomplished mechanically, as

in the CFSTR, or by gaseous bubbles, as in the SBCR. Although the rate of agitation is faster with a mechanical agitator than with bubbles, an agitator is undesirable in a highly corrosive medium such as an oxygen reactor due to the numerous internals required, such as the propeller, shaft, baffles, and other accessories that support the mixing system (Abdulrahman, 2016a).

Heating may be accomplished in two ways: indirectly or directly. The two most often used indirect procedures are to surround the vessel with a jacket or to use an inside coil. Direct heating may be accomplished by the use of gaseous bubbles and is more efficient than indirect heating, but is more complicated to scale up. The oxygen gas that exits the oxygen reactor at around 530°C may be heated to a higher temperature (such as 600°C) and then re-injected into the oxygen reactor from the bottom through a sparger. Direct contact heat transfer between the hot oxygen gas and the slurry within the oxygen reactor is possible in this instance (Abdulrahman, 2016a).

According to the comparison above, SBCR is more efficient in heat transmission than CFSTR but more difficult to scale up. However, with SBCR, thermal energy may be delivered to the reactor directly through gas bubbles, which can also be utilized to agitate the reactor's contents.

OXYGEN REACTOR SYSTEM DESCRIPTION

As with many chemical reactors, the oxygen reactor needs careful regulation of heat transfer to operate at peak efficiency. Cu_2OCl_2 decomposition into oxygen and molten CuCl is an endothermic process in the oxygen reactor, requiring a reaction heat of 129.2 kJ/mol and a temperature of 530°C, the highest temperature in the Cu-Cl cycle. As a result, heat must be provided to increase and maintain the temperature of the reactor's bulk (Ryskamp, 2004). The total amount of heat needed is the sum of reaction heat and the heat necessary to elevate the reactant temperature from 375°C (the temperature of solid particles formed during the hydrolysis process) to 530°C. The heat transfer coefficient, the difference between the bulk and surrounding temperatures of the heat transfer fluid (i.e., the driving force), and the size of the contact region where the heat transfer occurs all affect the heat transfer. Additionally, the heat transfer coefficient is dependent on the oxygen generation process's operating conditions, the physical qualities of the inventory materials, and the geometry of the equipment. Typically, this coefficient is established by the use of empirical correlations.

The oxygen reaction is a high temperature reaction that requires a source of high temperature heat. This heat may be generated by generation IV nuclear reactor designs such as the sodium-cooled reactor, the Canada Deuterium Uranium (CANDU) supercritical water reactor (CANDU-SCWR), Canada's Generation IV reactor, and the high temperature gas reactor (HTGR). While the first two reactors operate at lower temperatures (510°C – 625°C), they are ideally suited for matching a low temperature Cu-Cl thermochemical

cycle. However, coupling low temperature cycles to the HTGR (1000°C) may enable more cogeneration, resulting in much better hydrogen production efficiency. Solar energy is another non-polluting source of high-temperature heat.

In an indirect cycle system, an intermediate heat exchanger (IHX) is utilized to transmit heat from the main fluid in the nuclear reactor core to the secondary fluid, which then delivers the heat to the hydrogen plant's oxygen reactor. Helium, a nitrogen/helium combination, or a molten salt may be used as the secondary fluid. IHX is designed to collect heat from the main fluid at the maximum temperature achievable (the reactor output temperature) for use in the hydrogen generation process. Harvego (2006) studied several setups for an intermediate heat exchanger between a hydrogen generation cycle and an NGNP. The flow rates, temperature distribution across the loops, and other IHX needs were also suggested based on the design, and the reactor output temperature was set at 900°C in earlier research by Natesan et al. (2006).

MATERIAL PROPERTIES OF OXYGEN REACTOR

Ikeda and Kaye (2008), as well as Trevani et al. (2011), have investigated the thermochemical characteristics of copper oxychloride. Because copper oxychloride is not commercially accessible, these two investigations discovered strategies for its manufacture. Ikeda and Kaye (2008) used stoichiometric quantities of CuO and CuCl₂ in their approach. To prevent the presence of moisture, the procedure was carried out in a glove box filled with argon. Trevani et al. (2011) used a more straightforward method. Cu₂OCl₂ was created in their approach using a typical horizontal tube furnace equipped with a quartz tube and stainless-steel gas injection connectors. CuCl or CuCl₂ was placed into an alumina crucible and subjected for 48 hours to a flow of high-quality dry air at 370°C. The X-Ray Diffraction (XRD) analysis indicated that this approach produced very pure Cu₂OCl₂ samples. The approach is more scalable, and it is capable of producing the quantities necessary for large-scale oxygen generation tests. Cu₂OCl₂ is a solid that decomposes in the presence of water, hence it is essential to preserve it under nitrogen or dry air.

Parry (2008) reported calorimetric measurements of copper oxychloride's heat capacity in the range of 20-410°C. The Debye-Einstein technique was used to extrapolate thermodynamic data to 550°C. Uncertainty developed in the low-temperature range due to the quick change in heat capacity in this area. The slope of the calorimetric specific heat curve drops to less than 5 J/mol.K every 100°C above 400°C. Differences in observed data were attributed to undetected heat leakage. The standard deviation of results acquired using this approach was calculated to be 1.1%.

Abdulrahman (2016a, 2019a, 2020a) has derived a linear function of CuCl surface tension with temperature as follows:

$$\sigma_{\text{CuCl}} = 0.115 - 5.312 \times 10^{-5} T \quad (4)$$

The derivation was based on the approximate linear reduction of the surface tension with temperature and the equality of the surface tension to zero at the critical temperature of the liquid. The critical temperature that is used in deriving Eq. (4) is equal to 2435 K. The surface tension of molten CuCl in contact with air is equal to 0.092 N/m at the melting temperature of CuCl (430°C) (Janz and Tomkins, 1983).

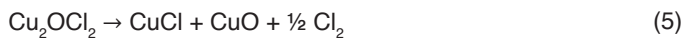
There are various obstacles and challenges in utilizing the real materials from the thermolysis reactor products in the experimental research for the scale up analysis (i.e. molten salt CuCl and oxygen gas). Abdulrahman (2016a, 2019a, 2020a) developed alternative materials by simulating the hydrodynamic and heat transport characteristics of actual materials utilizing dimensional analyses of the Buckingham pi theorem. These alternate materials have been identified as liquid water at a temperature of 22°C and helium gas at a temperature of 90°C. The physical properties for He gas and liquid water are shown in Table 1 (Abdulrahman, 2016a). Alternative materials offer a safe environment for experimental runs and operate at a lower temperature. Additionally, these materials are readily available and inexpensive. Abdulrahman's material simulation is a unique tool for assessing hydrodynamic and heat transport behaviours in a simulated environment prior to adaptation to the Cu-Cl cycle thermolysis reactor.

Physical Property	Unit	Gas Phase (He)	Liquid Phase (H ₂ O)
Temperature (T)	°C	90	22
Temperature (T)	K	363	295
Density (ρ)	kg/m ³	0.1344	998.2
Specific Heat (C_p)	J/kg K	5193	4182
Thermal Conductivity (k)	W/m K	0.1687	0.6
Dynamic Viscosity (μ)	kg/m s	2.267E-5	0.000975
Molecular Weight	kg/ kmol	4.0026	18.0152
Standard State Enthalpy	J/ kg mol	-	-2.858e+8
Surface Tension (σ)	N/m	-	0.0724

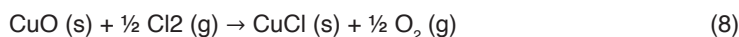
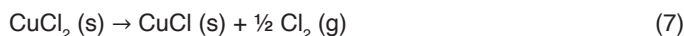
Table 1: Material properties for the Helium gas and liquid Water (Abdulrahman, 2016a).

OXYGEN PRODUCTION CHEMICAL REACTION

Experiments were carried out to determine the volatility of CuCl and the products of Cu₂OCl₂ decomposition. Copper oxychloride retained its chemical characteristics at temperatures up to 370°C. Cl₂ was released between 375°C and 470°C during the production of CuCl. Cl₂ then reacted with CuO to form oxygen and CuCl, as well as trace quantities of unreacted CuCl₂. Between 475°C and 550°C, XRD analysis demonstrated an increase in the quantity of CuCl₂ in the products, whereas the amount of CuO decreased. The decomposition reaction (called path I) has the following form:



Parallel to the competitive reaction, experimental data suggested that the secondary reaction was responsible for the partial drop in CuO caused by the Cl₂ generated in the former reaction. This collection was named “reaction “path I.” Another way to generate oxygen is by the decomposition of a combination of CuO and CuCl₂, as Serban et al. investigated (Serban et. al., 2004). The studies were conducted in a vertical reactor at 500°C using an equimolar combination of CuO and CuCl₂. The XRD measurement of the solid products revealed a pure CuCl solid phase. The investigation used a mechanistic approach and determined that oxygen evolution is constrained by CuCl₂ decomposition. As specified in the following equations “path II,” the reaction proceeded in two steps.



The competing reaction in Eq. (7) is cupric chloride’s heterogeneous and endothermic thermolysis. Even while only 60% decomposition of CuCl₂ occurs at 530°C, the addition of CuO seems to enhance decomposition. Additionally, it was found that the Cl₂ produced is completely consumed in the reaction with CuO, as indicated by Eq. (8), since no free Cl₂ was found in the gaseous products. The Gibbs free energy of the reaction suggests that it enters equilibrium around 500°C and then proceeds spontaneously, with increasing amounts of chlorine available to react with CuO as the temperature rises. However, experimental data suggested that CuCl₂ does not completely decompose until it reaches 600°C.

Lewis et al. (2005) utilized 40 mg of laboratory-produced Cu₂OCl₂ heated to 530°C for the oxygen generation process in their experiment. Based on the quantity of copper oxychloride used in the experiment, it was found that the observed mass of oxygen was more than the theoretical limit. The presence of chlorine peaks was found to be below background values. Lewis et al. (2003, 2019) utilized a stoichiometric combination of CuO and CuCl₂ heated to 500°C to achieve an oxygen output of 85%. The X-ray diffraction (XRD) analysis of products revealed the presence of CuCl and negligible levels of CuCl₂. At 500°C, 0.02 mol of an equimolar combination of CuO and dehydrated CuCl₂ was decomposed in a separate experiment. The oxygen production was more than what thermodynamic equilibrium studies expected. The amount of chlorine released was not determined. Continuous oxygen removal was used in the experiments. The XRD investigation of the solid products revealed the presence of CuCl and CuCl₂. The findings indicate that the oxygen released during copper oxychloride decomposition is more than the predicted yield from a combination of CuCl₂ and CuO. The reason chlorine was not found is unclear, however it might have been due to the presence of chlorine gas or a low yield of chlorine below the chlorine analyser’s detection threshold.

Marin (2012) established a novel experimental and theoretical basis for scaling up a $\text{CuO} \cdot \text{CuCl}_2$ decomposition reactor while considering the effect on the yield of the thermochemical copper-chlorine cycle for hydrogen production. He utilized a Stefan boundary condition in conjunction with a new particle model to monitor the location of the moving solid-liquid interface as the solid particle decomposes due to surface heat transfer. Thermo gravimetric Analysis (TGA) microbalance and laboratory scale batch reactor studies were used to investigate the conversion of $\text{CuO} \cdot \text{CuCl}_2$ and estimate the rate of endothermic reaction. At high temperatures and low Reynolds numbers, a second particle model finds characteristics that affect the transient chemical decomposition of solid particles embedded in a bulk fluid composed of molten and gaseous phases. For a particle suddenly submerged in a viscous continuum, the mass, energy, momentum, and chemical reaction equations were solved. Numerical solutions were generated and evaluated using experimental data on the chemical decomposition of copper oxychloride ($\text{CuO} \cdot \text{CuCl}_2$).

FACTORS AFFECTING OXYGEN REACTOR SIZE

There are many factors that affect oxygen reactor size. These factors include the residence time of the thermal decomposition for solid particles, terminal settling velocity of solid particles, production rate of hydrogen (mass balance), and reactor heating rate (heat balance) (Abdulrahman, 2016a, 2013a).

Terminal Settling Velocity of Particles

The amount of time it takes for solid particles to settle in a reactor with a limited volume is an essential metric to consider while designing the reactor (Felice and Kehlenbeck, 2000). The rate at which particles descend has a considerable impact on the height of the reactor. It is advised that the particle fall speed be kept as low as possible in order to provide adequate time for the decomposition process to be completed before reaching the bottom of the reactor. It is not necessary to have a high reactor in this situation.

Due to the fact that the density of the solid Cu_2OCl_2 particle is larger than that of molten CuCl , the falling velocity of a single particle under gravity will be greater than that of molten CuCl . The particle will continue to accelerate for a brief period and then descend at a constant velocity, where the effective weight of the particle and the drag force are identical. Thus, the most essential period is the period of constant-velocity descent (terminal settling velocity). The terminal velocity of solid particles is determined by a number of characteristics, including their size, shape (roundness), solid concentration and density, as well as the liquid's viscosity and density (Nguyen and Schulze, 2003).

Particle size: In industry, solid particles are often not uniform in size, but rather contain a variation of sizes. It is commonly established that bigger particles settle at a

faster rate than smaller ones. Baldi and Alaria (1978) indicated that when dealing with a distribution of particle sizes, it is appropriate to describe the particle diameter as the mass-mean diameter when computing the settling velocity.

Particle shape: In most theoretical computations, the form of solid particles is assumed to be spherical. The size of non-spherical particles may be described in terms of an equivalent volume of a sphere. A spherical particle's falling velocity is greater than that of a non-spherical particle with the same volume and density (Nguyen and Schulze, 2003).

Particle concentration: When a cloud of solid particles falls through a quiescent liquid, extra impeding actions have an impact on its falling velocity. These include the increased drag created by the close proximity of the particles inside the cloud and the liquid up flow induced by the falling particles. The impeding effects are highly dependent on the volumetric solid concentration in the cloud. The velocity of a hindered falling object is typically a fraction of the velocity of a free-falling object. For instance, with a solid concentration of 30% and a solid particle diameter range of 0.074-2 mm, the sand's impeded velocity is around 20%-40% of the single particle terminal velocity (Richardson and Zaki, 1954).

It is important to define in the design of the oxygen reactor's size if the settling velocity of the solid particles allows for sufficient residence time for complete decomposition of these particles before they settle to the reactor's bottom. It is widely established that the maximum settling velocity occurs when a single spherical particle falls infinitely deep into a fluid. Other factors such as particle shape, reactor wall, and impeding effects all contribute to the particles' settling velocity being reduced. The up-flow motion of the oxygen bubbles also reduces the fall of particles in the oxygen reactor.

Mass Production Rate of Hydrogen

In the design of any chemical reactor, it is necessary to study material balances (mass balances) which are based on the fundamental law of mass conservation. It is difficult to construct or run an oxygen reactor (or any other chemical plant) in a safe and cost-effective manner without proper material balances on hand. The general equation of the material balance is (Abdulrahman, 2016a, 2013a):

$$\frac{dm}{dt} = \dot{m}_i - \dot{m}_o + \dot{G} - \dot{C} \quad (9)$$

where: $\frac{dm}{dt}$ is the rate of change of the material m , \dot{m}_i and \dot{m}_o are the inlet and outlet mass flow rates respectively, \dot{G} and \dot{C} are the rate of generation and consumption respectively. Abdulrahman et al. (2016a, 2013a) investigated the flow material balance for continuous processes running in the steady state. To produce hydrogen, they have investigated the flow rates and chemical compositions of all streams entering and exiting

each individual piece of equipment in the Cu-Cl cycle. It has been shown that the flow rate of each component of the Cu-Cl cycle (in the event of full conversion of the components) changes linearly with the rate of hydrogen production throughout the cycle.

Using varying residence times and hydrogen production rates, it was possible to compute the optimal size of an oxygen reactor. It was discovered that the size of the oxygen reactor changes linearly with the rate of hydrogen production and the residence time. According to the findings of Abdulrahman et al. (2016a, 2013a), the minimal size of the oxygen reactor can be determined based on the mass balance of the Cu-Cl cycle, and the size is strongly influenced by the residence time and hydrogen production rate of the reactor. Also, the size of the oxygen reactor was anticipated to be large because of the presence of copper (Cu), which has the maximum molecular weight of 63.54 g/mol in the Cu-Cl cycle, and hence the largest molecular weight in the Cu-Cl cycle.

METHOD OF HEATING OXYGEN REACTOR

A suitable method of heating the oxygen reactor is needed to provide enough heat that is necessary for solid decomposition. Heating the $\text{Cu}_2\text{OCl}_2(\text{s})$ particles only is undesirable, because of relatively slow rate of heat transfer. A more practical and efficient option is to heat the molten salt inside the oxygen reactor to in turn transfer the heat within the reactor from the liquid (molten CuCl) to the solid Cu_2OCl_2 (reactant) particles. The molten salt bath can be sustained by the reaction product itself. This approach is the most applicable and recommended one.

Due to buoyancy of the gas in the molten salt, the oxygen product will leave the reactant particles immediately. This fast separation aids to minimize heat transfer resistance to the reactant particles, which then helps make the overall reaction rate closer to the intrinsic reaction rate. The design of the reactor requires a high efficiency of heat exchange and separation of reactant (solid particles) from products, as well as one product (oxygen) from another (molten salt).

There are two main heating methods for reactor: electrical heating and fluid heating. The main disadvantage of electrical heating is the limited efficiency of electricity generation from nuclear heat (currently less than 35%). A more suitable method is to heat the molten salt by using a heating fluid (such as helium gas or molten salt) without using electricity.

Two main configurations of molten salt heating by a fluid can be used: direct and indirect heating. Direct heating places the heating fluid in direct contact with the heated medium. The advantage of heating directly is that, heating fluid is nearly 100% efficient with this method. This is because all heat that is generated is absorbed directly by the process. This helps to speed heat-up and eliminate thermal lag. There is no intermediate heat transfer medium that could result in heat losses. Direct heating can be applied by using a Slurry Bubble Column Reactor (SBCR), where the heating gas can be introduced to the reactor from the bottom through a sparger.

Indirect reactor heating uses a heat transfer medium to deliver the heat to the reactor vessel. Indirect methods can be external heating of the reactor using the reactor wall (or immersed tubes walls). There are various advantages of indirect heating. The biggest advantage is that the heating fluid can typically be serviced without draining the reactor. Second, indirect heating often allows watt density exposed to the process fluid, which is the number of watts concentrated per unit surface area of process side, to be lowered by spreading the heat over a larger surface. Finally, overheat conditions can be limited in many instances by simply limiting the temperature of the heat transfer medium, so that the process fluid is never exposed to temperatures higher than the heat transfer fluid temperature.

In spite of the above advantages, the disadvantages of indirect heating may be critical to the oxygen production process. The primary disadvantage is the thermal lag caused by using a heat transfer medium to carry the heat such as the reactor wall. The delay is caused by the fact that the heating fluid must first heat the heat transfer medium before the heat transfer medium can heat the process. If there is a large mass of heat transfer medium, larger heating capacities will be required to raise the temperatures.

Different types of indirect heat transfer surfaces can be used in an industrial oxygen reactor such as jackets, helical tubes immersed directly inside the reactor and vertical tube baffles (Oldshue, 1983). A reactor jacket is usually adequate to provide the required heat transfer surface for low and moderate heat duties (in terms of heat duty per unit of vessel volume). As heat duty increases, internal heat transfer surfaces (helical coils, baffle pipes, or plate coils) may be required.

Indirect Heat Transfer of the Oxygen Reactor

Thermal scaling up of the three-phase oxygen generation reactor in the Cu-Cl cycle was investigated using indirect heat transfer techniques (Abdulrahman, 2016a, 2016b, 2016c, 2019b, 2019c, 2013b, 2022a). The size of the oxygen reactor necessary to generate sufficient heat input was investigated in these researches for various hydrogen generation rates. The researches employed a continuous stirred tank reactor (CSTR) that was heated by a half pipe jacket (Abdulrahman, 2016a, 2016b) or an internal helical tube (Abdulrahman, 2016a, 2016c). The thermal resistance of each part of the reactor system was investigated in order to determine its influence on the reactor's heat balance. The system thermal resistance was found to be dominated by the reactor wall in jacketed reactors (Abdulrahman, 2016a, 2016b), and by the helical tube wall and service side in oxygen reactor systems with an internal helical tube (Abdulrahman, 2016a, 2016c).

The Cu-Cl cycle was assumed to be powered by a nuclear reactor in the above studies, and two different kinds of nuclear reactors were considered as a heat source for the oxygen reactor. The CANDU Super Critical Water Reactor (CANDU-SCWR) and the High Temperature Gas Reactor (HTGR) were two of these designs. It was established that a

larger heat transfer rate is required for CANDU-SCWR by three to four times that of HTGR, due to the HTGR's higher exit temperature, which results in greater temperature differential between the service and process sides than the SCWR.

From a thermal balancing standpoint, the impacts of reactor diameter and aspect ratio on the size of the oxygen reactor were calculated. It was determined that the size of the oxygen reactor reduces nonlinearly when the reactor diameter or aspect ratio increases, with the reactor diameter having a greater influence on the reactor size than the aspect ratio. The pace at which the oxygen reactor's size decreases was discovered to be slowed by increasing the reactor's diameter or aspect ratio.

On the service side, several kinds of working fluids were employed, including helium gas and CuCl molten salt, and their properties were compared. There is no discernible variation in the size of the jacketed oxygen reactor whether helium gas or CuCl molten salt is used (Abdulrahman, 2016a, 2016b). Due to the decrease in the number of oxygen reactors, it was established that utilizing CuCl molten salt in the service side is thermally superior to using helium gas in the oxygen reactor using an internal helical tube for heating (Abdulrahman, 2016a, 2016c). In general, both helium gas and CuCl molten salt have technical concerns, and both should be preserved and investigated until these technical difficulties are answered and an optimum decision can be chosen.

The findings of heat transfer studies conducted on the oxygen reactor with an internal helical tube were compared to the results of material balances and heat transfer analyses conducted on the oxygen reactor with a half pipe jacket. Due to the increased size needed for the heat balance, it was discovered that the size of the oxygen reactor is dictated by the heat balance rather than the material balance. Additionally, it was shown that delivering heat to the oxygen reactor through an internal helical tube is more efficient than utilizing a half pipe jacket.

Direct Contact Heat Transfer of the Oxygen Reactor

In examining the direct contact heat transfer within the oxygen reactor, comprehensive investigations were conducted utilizing both experimental and computational fluid dynamics (CFD) approaches (Abdulrahman, 2015, 2016a, 2016d, 2016e, 2016f, 2016g, 2018, 2020b,, 2020c, 2022b, 2022c, 2022d, 2023a, 2023b, 2023c). These studies aimed to understand and analyse the heat transfer mechanisms occurring within the reactor, where oxygen gas interacts directly with the other components, such as molten salt or solid particles.

The experimental studies involved setting up physical models of the oxygen reactor and conducting tests under controlled conditions to observe and measure the heat transfer rates, temperature profiles, and other relevant parameters. These experiments provided valuable data on how heat is transferred in the reactor, the influence of various operating conditions, and the effects of different reactor designs on the efficiency of heat transfer.

Concurrently, CFD studies were carried out to simulate the heat transfer processes within the oxygen reactor. Using Ansys Fluent software, detailed models of the reactor were created, incorporating the physical and chemical properties of the materials involved. These simulations allowed for a deeper analysis of the heat transfer phenomena, including the visualization of temperature distributions, gas holdup and flow patterns.

By combining the insights gained from both experimental and CFD studies, researchers aimed to optimize the design and operation of the oxygen reactor for improved heat transfer performance. This holistic approach ensures a more accurate and comprehensive understanding of the direct contact heat transfer mechanisms in the oxygen reactor, which is crucial for the development of more efficient and effective thermochemical processes for oxygen production.

Experimental Studies

Scaling up the thermolysis reactor requires a thorough understanding of hydrodynamics and heat transfer. However, using the actual products of the thermolysis reactor, such as molten salt CuCl and oxygen gas, presents several challenges in experimental studies on scaling up. These challenges include: 1) the high melting temperature of cuprous chloride (CuCl) at 430°C, 2) the non-transparent dark grey colour of molten CuCl, which obstructs the visibility of oxygen bubbles, 3) the highly corrosive nature of molten cuprous chloride, 4) the strong oxidizing property of oxygen gas, which can lead to rapid combustion of materials, and 5) the high-temperature process involved. To overcome these challenges, alternative materials have been identified using dimensional analysis to simulate the hydrodynamic and heat transfer behaviours of the actual materials. Liquid water at $22\pm 2^\circ\text{C}$ and helium gas at $90\pm 2^\circ\text{C}$ have been found to be suitable substitutes. These alternative materials not only provide a safer environment for experiments but also allow for lower operating temperatures. Moreover, they are readily available and more cost-effective (Abdulrahman, 2019a, 2020a).

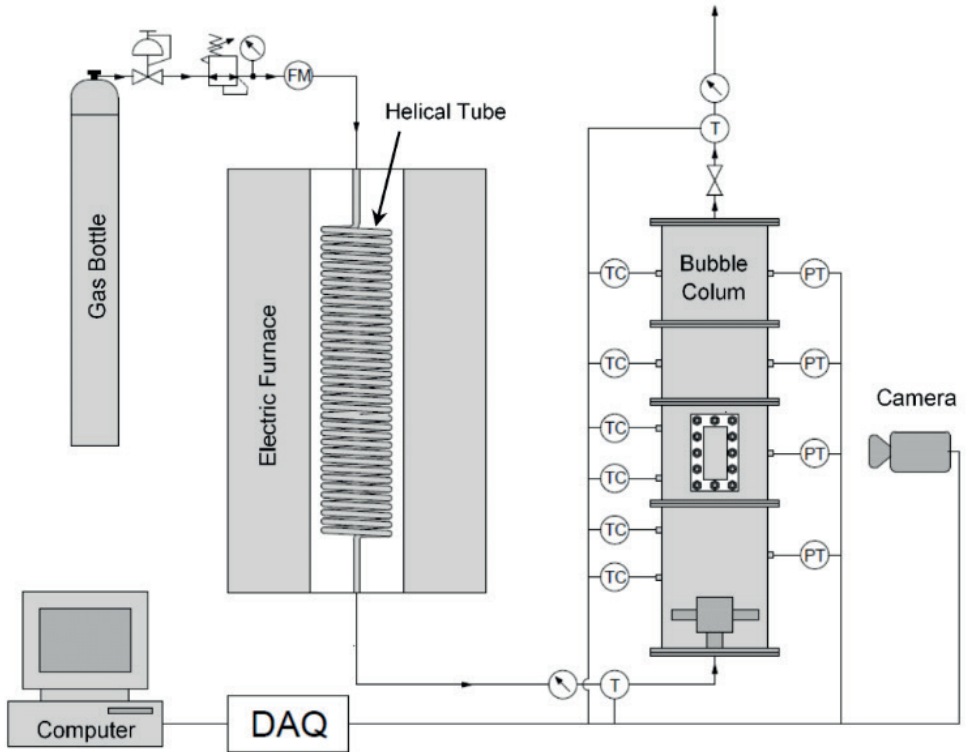
The experimental studies of the oxygen reactor have shed light on key aspects of SBCRs, including transition velocity, overall gas holdup, and direct contact heat transfer, providing valuable insights for optimizing their performance (Abdulrahman, 2015, 2016a, 2016d, 2016e, 2018). In the study of the transition velocity, which marks the shift from homogeneous to churn turbulent flow regimes within the reactor, the experiments revealed that the transition velocity decreases with an increase in static liquid height and solid concentration. This finding suggests that the physical dimensions of the reactor and the density of the slurry play significant roles in determining the flow regime. Also, the research indicated that slug flow, a regime characterized by large gas bubbles, is not typically present in industrial SBCRs (Abdulrahman, 2016e).

Another important aspect investigated experimentally is the overall gas holdup, which refers to the volume fraction of gas within the reactor. This parameter is crucial for

assessing the reactor's efficiency and capacity for mass transfer. The experimental study found that the overall gas holdup increases with the superficial gas velocity, particularly at lower velocities. However, it decreases with increasing static liquid height and solid concentration. Interestingly, the impact of solid particle diameter on gas holdup was found to be negligible, suggesting that particle size might not be a critical factor in certain operating conditions (Abdulrahman, 2016d).

Direct contact heat transfer in SBCRs, is a process vital for maintaining optimal reaction temperatures and energy efficiency. The experimental results showed that both the volumetric heat transfer coefficient and the slurry temperature increase with the superficial gas velocity, with a more pronounced effect at lower velocities. Conversely, these parameters decrease with an increase in static liquid height and solid concentration. The findings imply that manipulating the gas flow rate and reactor dimensions can effectively control heat transfer within the system (Abdulrahman, 2015). The schematic diagram of the SBC experimental setup is illustrated in Fig.1 and the dimensions of the reactor column and sparger used in the experiments are shown in Figs. 2 and 3 respectively.

The experimental studies provide a deeper understanding of the complex dynamics within slurry bubble column reactors. By elucidating the relationships between key operating parameters and reactor performance, these findings offer valuable guidance for designing and optimizing SBCRs in various industrial applications. For instance, adjusting the static liquid height and solid concentration can help regulate the transition velocity and gas holdup, while controlling the superficial gas velocity can optimize heat transfer efficiency.





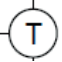

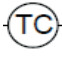
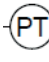


- | | | | |
|---|----------------------------------|---|--------------------------------|
|  | Pressure Regulator of Gas Bottle |  | Pressure Regulator |
|  | Thermocouple (Inlet & Outlet) |  | Pressure Gage (Inlet & Outlet) |
|  | Thermocouple (Reactor) |  | Pressure Transducer |
|  | Digital Flow Meter |  | Globe Valve |

Fig. 1 Schematic diagram of the experimental setup (Abdulrahman, 2016a).

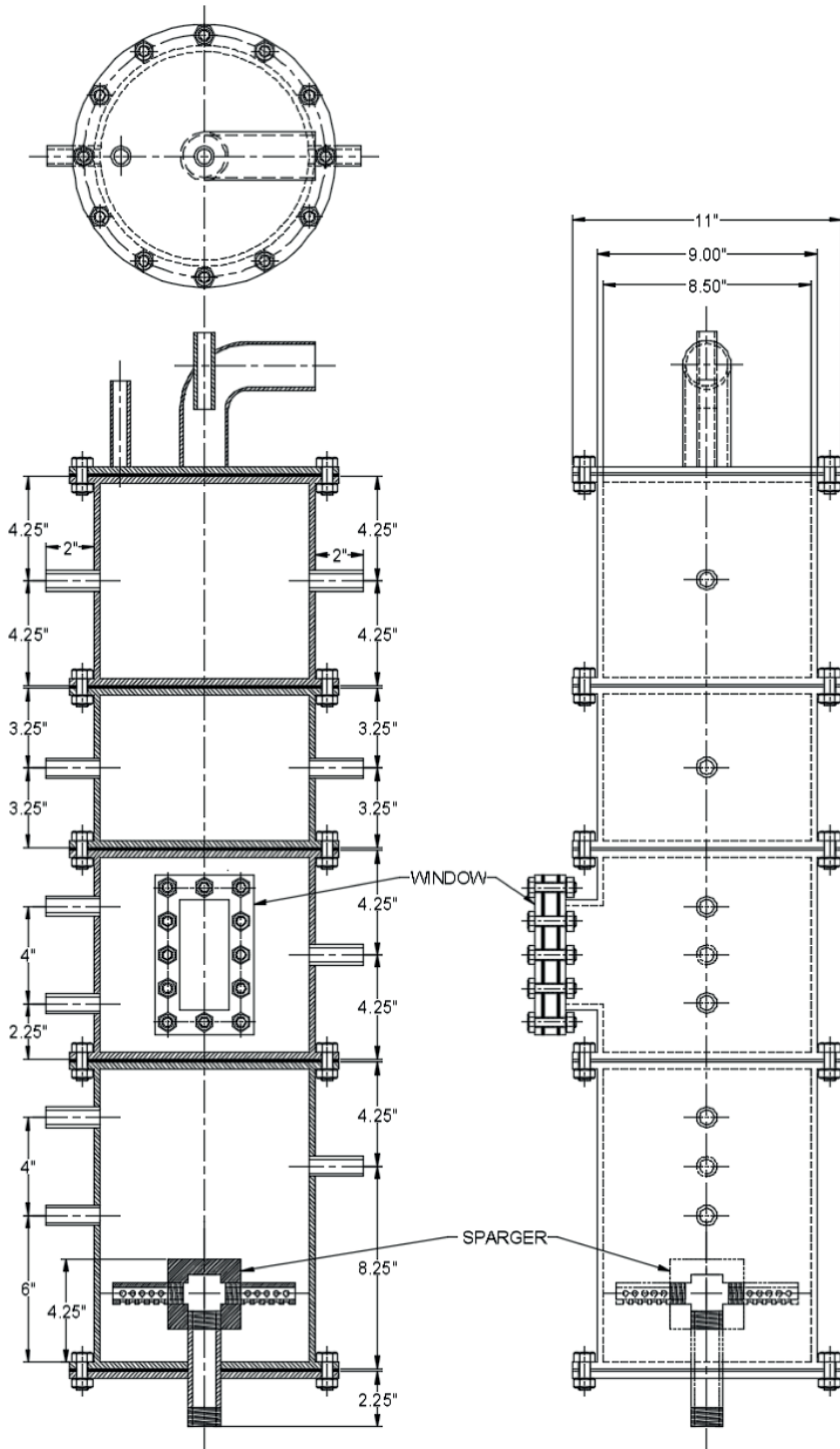


Fig. 2 Reactor column dimensions (Abdulrahman, 2016a).

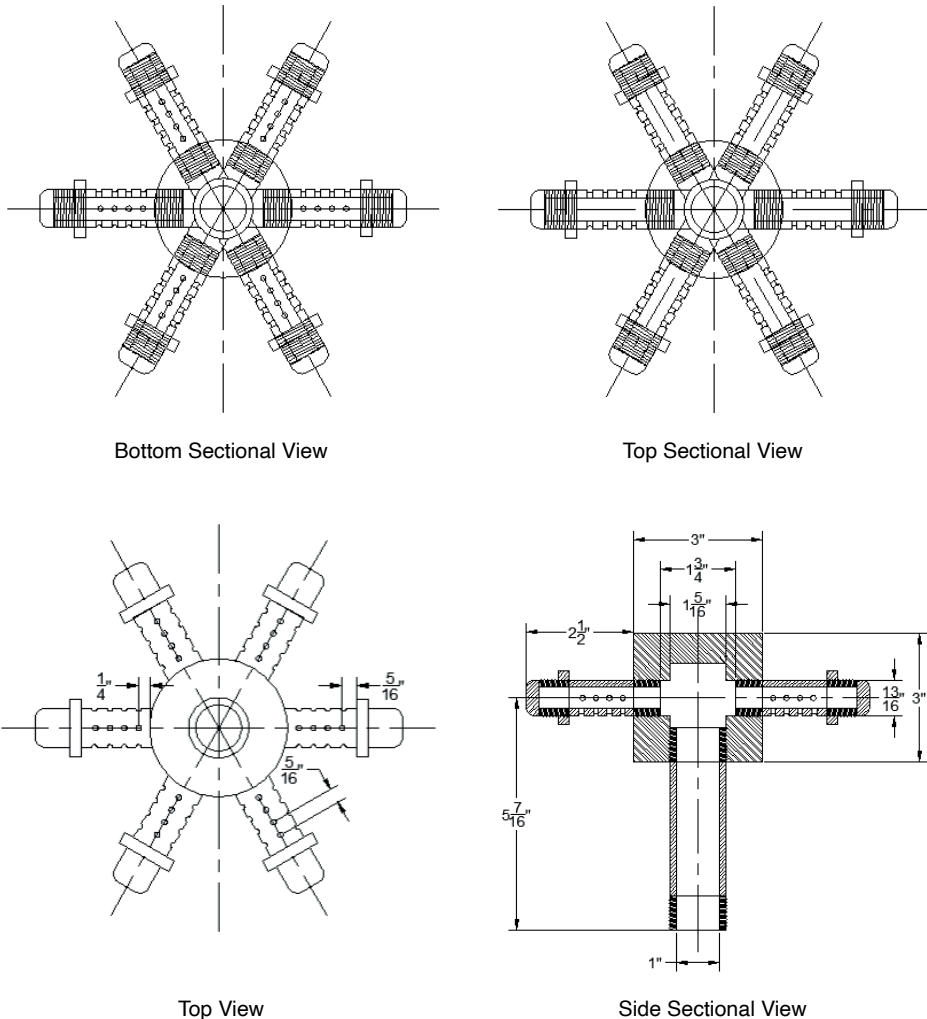


Fig. 3 Dimensions of the sparger (Abdulrahman, 2016a).

CFD Studies

The objective of the Computational Fluid Dynamics (CFD) simulations of direct contact heat transfer in the multiphase oxygen reactor, is to enhance our understanding of the hydrodynamics and heat transfer phenomena within these reactors. A comprehensive review of Eulerian CFD approaches for analysing BCR/SBCRs has highlighted the accuracy of these models in predicting reactor performance. Key findings include the increase in gas holdup with superficial gas velocity, column pressure, and gas phase density, and the uneven distribution of gas holdup within the reactor (Abdulrahman, 2022d).

One area of focus in CFD studies, is the volumetric heat transfer coefficient in SBCRs, where helium gas is injected through a slurry of water and alumina solid particles.

Researchers have investigated the effects of superficial gas velocity, static liquid height, and solid particle concentration on the volumetric heat transfer coefficient. CFD simulations revealed that the heat transfer coefficient increases with superficial gas velocity and decreases with higher static liquid height or solid concentration. These findings are crucial for optimizing reactor design and operation for efficient heat transfer (Abdulrahman, 2016f).

Temperature distribution within the slurry is another aspect that has been explored through 2D CFD simulations. Similar to the heat transfer coefficient, the average slurry temperature rises with increased superficial gas velocity and drops with higher static liquid height or solid concentration. However, the impact of solid concentration on temperature is found to be negligible. These insights are valuable for maintaining optimal reactor temperatures for various chemical processes (Abdulrahman, 2016g, 2020b, 2020c, 2022b).

Finally, the overall gas holdup in helium-water bubble columns has also been predicted using 2D and 3D CFD simulations. Results indicate that gas holdup increases with superficial gas velocity and decreases with higher static liquid height. The three-dimensional model was found to be more accurate for gas holdup in comparison to the two-dimensional model. This information is essential for scaling up bubble column reactors, as gas holdup is a key parameter describing reactor performance (Nassar, 2023; Abdulrahman & Nassar, 2023a, 2023b, 2023c).

In Table 2, the equations utilized in the CFD analysis are displayed. Table 2 contains equations that are explicitly expressed in gas phase. Since the equations for the liquid phase are comparable to those for the gas phase, they are not repeated. Table 3 summarizes the setup used in the simulations.

Description	Equation
Volume equation (Abdulrahman, 2019c)	$V_g = \int_V \alpha_g dV$
Continuity equation in 3D Polar coordinates (r, θ, y) (Harvego, 2006)	$\nabla \cdot \mathbf{V}_g = \frac{\partial v_{r,g}}{\partial r} + \frac{v_{r,g}}{r} + \frac{1}{r} \frac{\partial v_{\theta,g}}{\partial \theta} + \frac{\partial v_{y,g}}{\partial y} = 0$
Momentum equation in 3D Polar coordinates (Harvego, 2006)	$\rho_g \alpha_g \left(\frac{\partial v_r}{\partial t} + v_r \frac{\partial v_r}{\partial r} + \frac{v_\theta}{r} \frac{\partial v_r}{\partial \theta} + v_y \frac{\partial v_r}{\partial y} - \frac{v_\theta^2}{r} \right) = -\alpha_g \frac{\partial P}{\partial r} + \alpha_g \frac{\mu_{g,eff}}{3} \frac{\partial(\nabla \cdot \mathbf{V})}{\partial r} + \mu_{g,eff} \alpha_g \left[\frac{1}{r} \frac{\partial}{\partial r} \left(r \frac{\partial v_r}{\partial r} \right) + \frac{1}{r^2} \frac{\partial^2 v_r}{\partial \theta^2} + \frac{\partial^2 v_r}{\partial y^2} - \frac{v_r}{r^2} - \frac{2}{r^2} \frac{\partial v_\theta}{\partial \theta} \right] + \rho_g \alpha_g g_r + M_{i,g,r}$
	$\rho_g \alpha_g \left(\frac{\partial v_\theta}{\partial t} + v_r \frac{\partial v_\theta}{\partial r} + \frac{v_\theta}{r} \frac{\partial v_\theta}{\partial \theta} + v_y \frac{\partial v_\theta}{\partial y} + \frac{v_r v_\theta}{r} \right) = -\alpha_g \frac{1}{r} \frac{\partial P}{\partial \theta} + \alpha_g \frac{\mu_{g,eff}}{3r} \frac{\partial(\nabla \cdot \mathbf{V})}{\partial \theta} + \alpha_g \mu_{g,eff} \left[\frac{1}{r} \frac{\partial}{\partial r} \left(r \frac{\partial v_\theta}{\partial r} \right) + \frac{1}{r^2} \frac{\partial^2 v_\theta}{\partial \theta^2} + \frac{\partial^2 v_\theta}{\partial y^2} + \frac{2}{r^2} \frac{\partial v_r}{\partial \theta} - \frac{v_\theta}{r^2} \right] + \rho_g \alpha_g g_\theta + M_{i,g,\theta}$
	$\rho_g \alpha_g \left(\frac{\partial v_y}{\partial t} + v_r \frac{\partial v_y}{\partial r} + \frac{v_\theta}{r} \frac{\partial v_y}{\partial \theta} + v_y \frac{\partial v_y}{\partial y} \right) = -\alpha_g \frac{\partial P}{\partial y} + \alpha_g \mu_{g,eff} \left[\frac{1}{r} \frac{\partial}{\partial r} \left(r \frac{\partial v_y}{\partial r} \right) + \frac{1}{r^2} \frac{\partial^2 v_y}{\partial \theta^2} + \frac{\partial^2 v_y}{\partial y^2} \right] + \rho_g \alpha_g g_y + M_{i,g,y}$
Energy equation in 3D Polar coordinates (Harvego, 2006)	$\alpha_g \rho_g C \left(\frac{\partial T_g}{\partial t} + v_{r,g} \frac{\partial T_g}{\partial r} + \frac{v_{\theta,g}}{r} \frac{\partial T_g}{\partial \theta} + v_{y,g} \frac{\partial T_g}{\partial y} \right) = \bar{\tau}_g : \nabla \mathbf{V}_g + k_g \left(\frac{1}{r} \frac{\partial}{\partial r} \left(r \frac{\partial T_g}{\partial r} \right) + \frac{1}{r^2} \frac{\partial^2 T_g}{\partial \theta^2} + \frac{\partial^2 T_g}{\partial y^2} \right) + S_g + Q_{g,sl}$
Effective density	$\hat{\rho}_g = \alpha_g \rho_g$
Drag force (Abdulrahman, 2019c)	$M_D = \frac{\rho_g f}{6 \tau_b} d_b A_i (\mathbf{V}_g - \mathbf{V}_l)$
Interfacial area (Abdulrahman, 2019c)	$A_i = \frac{6 \alpha_g (1 - \alpha_g)}{d_b}$
Schiller-Naumann drag equation (Abdulrahman, 2013b)	$C_D = \begin{cases} \frac{24(1+0.15 Re_b^{0.687})}{Re_b} & Re_b \leq 1000 \\ 0.44 & Re_b > 1000 \end{cases}$

Table 2: Details of equations used in the 3D CFD simulations (Abdulrahman & Nassar, 2023a).

General	<i>Solver Type</i>	Pressure-Based		
	<i>Velocity Formulation</i>	Absolute		
	<i>Time</i>	Steady		
	<i>Gravity</i>	ON		
Models	Multiphase-Eulerian			
	Energy-On			
	Viscous-Standard $k - \epsilon$, Standard Wall Function, Dispersed			
Materials	Water liquid			
	Helium gas			
Phases	Primary phase=liquid phase			
	Secondary Phase=gas phase			
Bubble Diameter	Sauter-mean diameter			
Solution Methods	<i>Scheme</i>	Phase-Coupled SIMPLE		
	<i>Spatial Discretization</i>	Gradient	Least Squares Cell Based	
		Momentum	Second Order Upwind	
		Volume Fraction	First Order Upwind	
		Turbulent Kinetic Energy	Second Order Upwind	
		Turbulent Dissipation Rate	Second Order Upwind	
		Energy	Second Order Upwind	
		Interfacial Area Concentration	Second Order Upwind	

Table 2 Summary of the SBCR problem setup (Abdulrahman, 2016f).

In conclusion, CFD simulations have provided valuable insights into the hydrodynamics and heat transfer in slurry bubble column reactors. These advancements are instrumental in optimizing reactor designs and operations for various industrial applications, particularly in hydrogen production, contributing to the development of sustainable energy technologies. The results of both the experimental and CFD works are shown in Table 4.

Volumetric Heat Transfer Coefficient	Average Slurry Temperature	Overall Gas Holdup	Transition Velocity
Increases by increasing the superficial gas velocity with a higher rate of increase at lower superficial gas velocity.			In the industrial SBCRs, the slug flow regime does not exist and there is only one transition velocity, which is between the homogeneous and heterogeneous flow regimes.
Decreases by increasing the static liquid height.			
Decreases by increasing solid concentration.	The decrease of the slurry temperature with the solid concentration is negligible.	Decreases by increasing solid concentration and at a higher solid concentration, the changing rate of the overall gas holdup with the superficial gas velocity and/or the solid concentration is lower. The effect of the solid particle diameter on overall gas holdup is negligible.	Decreases by increasing solid concentration.
The rate of decrease with the solid concentration are approximately the same for different superficial gas velocities.		The distribution along the cross-section of the column is unequal, where the gas holdup is higher at the centre of the column and lower near the wall region.	
Profiles calculated from CFD models, generally under-predicted the experimental data of Abdulrahman (2015, 2016d, 2016f).			
The CFD models correctly predicted the effects of superficial gas velocity, static liquid height and solid concentration.			
The CFD results were validated for superficial gas velocities up to 0.15 m/s, and aspect ratios up to 4.			

Table 4: Results of experimental and CFD analyses for direct contact heat transfer (Abdulrahman, 2022c).

CONCLUSIONS

Recent improvements in the multiphase oxygen reactor for the copper-chlorine thermochemical cycle were presented and assessed in this review work. The study identified previous experimental and theoretical findings acquired from research groups working on the development of scaled-up oxygen reactor facilities. The oxygen reactor's type and description were discussed in details and it is concluded that using SBCR is the best option for the oxygen reactor. Oxygen production chemical reaction was described in details and it was found that the reaction is an endothermic reaction with a reaction heat of 129.2 kJ/mol and a temperature of 530°C which is the highest temperature in the Cu-Cl

cycle. The source of heat can be from nuclear reactors or solar energy sources. Also, the material properties of the oxygen reactor contents were extensively explained. Moreover, the factors that affect the size of the oxygen reactor were discussed. The factors include the residence time of the thermal decomposition for solid particles, terminal settling velocity of solid particles, production rate of hydrogen, and reactor heating rate. The techniques of heat transfer required by the oxygen reactor, such as indirect and direct contact heat transfer, were also analysed in this study. It was concluded that using direct contact heat transfer is preferred to indirect heat transfer methods.

REFERENCES

Abdulrahman, M. W. (2015). **Experimental studies of direct contact heat transfer in a slurry bubble column at high gas temperature of a helium–water–alumina system.** *Applied Thermal Engineering*, 91, 515-524.

Abdulrahman, M. W. (2016a). **Analysis of the thermal hydraulics of a multiphase oxygen production reactor in the Cu-Cl cycle.** University of Ontario Institute of Technology (Canada).

Abdulrahman, M. W. (2016b). **Similitude for thermal scale-up of a multiphase thermolysis reactor in the cu-cl cycle of a hydrogen production.** *World Academy of Science, Engineering and Technology, International Journal of Electrical, Computer, Energetic, Electronic and Communication Engineering*, 10(5), 567-573.

Abdulrahman, M. W. (2016c). **Heat transfer analysis of a multiphase oxygen reactor heated by a helical tube in the cu-cl cycle of a hydrogen production.** *World Academy of Science, Engineering and Technology, International Journal of Mechanical, Aerospace, Industrial, Mechatronic and Manufacturing Engineering*, 10(6), 1018-1023.

Abdulrahman, M. W. (2016d). **Experimental studies of gas holdup in a slurry bubble column at high gas temperature of a helium– water– alumina system.** *Chemical Engineering Research and Design*, 109, 486-494.

Abdulrahman, M. W. (2016e). **Experimental studies of the transition velocity in a slurry bubble column at high gas temperature of a helium–water–alumina system.** *Experimental Thermal and Fluid Science*, 74, 404-410.

Abdulrahman, M. W. (2016f). **CFD simulations of direct contact volumetric heat transfer coefficient in a slurry bubble column at a high gas temperature of a helium–water–alumina system.** *Applied thermal engineering*, 99, 224-234.

Abdulrahman, M. W. (2016g). **CFD Analysis of Temperature Distributions in a Slurry Bubble Column with Direct Contact Heat Transfer.** In *Proceedings of the 3rd International Conference on Fluid Flow, Heat and Mass Transfer (FFHMT'16)*.

Abdulrahman, M. W. (2018). *U.S. Patent No. 10,059,586*. Washington, DC: U.S. Patent and Trademark Office.

Abdulrahman, M. W. (2019a). **Simulation of Materials Used in the Multiphase Oxygen Reactor of Hydrogen Production Cu-Cl Cycle.** In *Proceedings of the 6 the International Conference of Fluid Flow, Heat and Mass Transfer (FFHMT'19)* (pp. 123-1).

- Abdulrahman, M. W. (2019b). **Heat transfer in a tubular reforming catalyst bed: Analytical modelling.** In *proceedings of the 6th International Conference of Fluid Flow, Heat and Mass Transfer*.
- Abdulrahman, M. W. (2019c). **Exact analytical solution for two-dimensional heat transfer equation through a packed bed reactor.** In *Proceedings of the 7th World Congress on Mechanical, Chemical, and Material Engineering*.
- Abdulrahman, M. W. (2020a). *U.S. Patent No. 10,526,201*. Washington, DC: U.S. Patent and Trademark Office.
- Abdulrahman, M. W. (2020b). **Effect of Solid Particles on Gas Holdup in a Slurry Bubble Column.** In *Proceedings of the 6th World Congress on Mechanical, Chemical, and Material Engineering*.
- Abdulrahman, M. W. (2020c). **CFD Simulations of Gas Holdup in a Bubble Column at High Gas Temperature of a Helium-Water System.** In *Proceedings of the 7th World Congress on Mechanical, Chemical, and Material Engineering (MCM'20)* (pp. 169-1).
- Abdulrahman, M. W. (2022a). **Heat Transfer Analysis of the Spiral Baffled Jacketed Multiphase Oxygen Reactor in the Hydrogen Production Cu-Cl Cycle.** In *Proceedings of the 9th International Conference on Fluid Flow, Heat and Mass Transfer (FFHMT'22)*.
- Abdulrahman, M. W. (2022b). **Temperature profiles of a direct contact heat transfer in a slurry bubble column.** *Chemical Engineering Research and Design*, 182, 183-193.
- Abdulrahman, M. W. (2022c). **Review of the Thermal Hydraulics of Multi-Phase Oxygen Production Reactor in the Cu-Cl Cycle of Hydrogen Production.** In *Proceedings of the 9th International Conference on Fluid Flow, Heat and Mass Transfer (FFHMT'22)*.
- Abdulrahman, M. W., & Nassar, N. (2022d). **Eulerian Approach to CFD Analysis of a Bubble Column Reactor—A Review.** In *Proceedings of the 8th World Congress on Mechanical, Chemical, and Material Engineering (MCM'22)*.
- Abdulrahman, M. W., & Nassar, N. I. (2023a). **A Three-Dimensional CFD Analyses for the Gas Holdup in a Bubble Column Reactor.** In *Proceedings of the 9th World Congress on Mechanical, Chemical, and Material Engineering (MCM'23)*.
- Abdulrahman, M. W., & Nassar, N. I. (2023b). **Three Dimensional CFD Analyses for the Effect of Solid Concentration on Gas Holdup in a Slurry Bubble Column.** In *Proceedings of the 9th World Congress on Mechanical, Chemical, and Material Engineering (MCM'23)*.
- Abdulrahman, M. W., & Nassar, N. I. (2023c). **Effect of Static Liquid Height on Gas Holdup of a Bubble Column Reactor.** In *Proceedings of the 9th World Congress on Mechanical, Chemical, and Material Engineering (MCM'23)*.
- Abdulrahman, M. W., Wang, Z., & Naterer, G. F. (2013a). **Scale-up analysis of three-phase oxygen reactor in the Cu-Cl thermochemical cycle of hydrogen production.** In *EIC Climate Change Technology Conference*.
- Abdulrahman, M. W., Wang, Z., Naterer, G. F., & Agelin-Chaab, M. (2013b). **Thermohydraulics of a thermolysis reactor and heat exchangers in the Cu-Cl cycle of nuclear hydrogen production.** In *Proceedings of the 5th World Hydrogen Technologies Convention*.

- Baldi, G., Conti, R., & Alaria, E. (1978). **Complete suspension of particles in mechanically agitated vessels.** *Chemical Engineering Science*, 33(1), 21-25.
- De Micco, G., Bohé, A. E., & Pasquevich, D. M. (2007). **A thermogravimetric study of copper chlorination.** *Journal of alloys and compounds*, 437(1-2), 351-359.
- Di Felice, R., & Kehlenbeck, R. (2000). **Sedimentation velocity of solids in finite size vessels.** *Chemical Engineering & Technology: Industrial Chemistry-Plant Equipment-Process Engineering-Biotechnology*, 23(12), 1123-1126.
- Forsberg, C. W. (2007). **Future hydrogen markets for large-scale hydrogen production systems.** *International Journal of Hydrogen Energy*, 32(4), 431-439.
- Harvego, E. A. (2006). **Evaluation of next generation nuclear power plant (NGNP) intermediate heat exchanger (IHX) operating conditions (No. INL/EXT-06-11109).** Idaho National Lab.(INL), Idaho Falls, ID (United States).
- Ikeda, B. M., & Kaye, M. H. (2008, August). **Thermodynamic properties in the Cu-Cl-OH system.** In *7th International conference on nuclear and radiochemistry, Budapest, Hungary.*
- Janz, G. J., & Tomkins, R. P. T. (1983). Molten salts: volume 5, Part 2. **Additional single and multi-component salt systems. Electrical conductance, density, viscosity and surface tension data.** *Journal of physical and chemical reference data*, 12(3), 591-815.
- Lewis, M. A., Masin, J. G., & Vilim, R. B. (2005). **Development of the low temperature Cu-Cl thermochemical cycle.** *Argonne National Laboratory, International Congress on Advances in Nuclear Power Plants*, Seoul, Korea.
- Lewis, M. A., Serban, M., & Basco, J. K. (2003). **Generating hydrogen using a low temperature thermochemical cycle.** In *Proceedings of the ANS/ENS 2003 Global International Conference on Nuclear Technology, New Orleans.*
- Li, X., Zhang, L., Nakaya, M., & Takenaka, A. (2016, October). **Application of economic MPC to a CSTR process.** In *2016 IEEE Advanced Information Management, Communicates, Electronic and Automation Control Conference (IMCEC)* (pp. 685-690). IEEE.
- Marin, G. D. (2012). **Kinetics and transport phenomena in the chemical decomposition of copper oxychloride in the thermochemical Cu-Cl Cycle** (Doctoral dissertation).
- Nassar, N. I. (2023). **A Three-Dimensional CFD Analyses for the Hydrodynamics of the Direct Contact Heat Transfer in the Oxygen Production Slurry Bubble Column Reactor of the Cu-Cl Cycle of Hydrogen Production.** Rochester Institute of Technology.
- Natesan, K., Moisseytsev, A., & Majumdar, S. (2009). **Preliminary issues associated with the next generation nuclear plant intermediate heat exchanger design.** *Journal of nuclear materials*, 392(2), 307-315.
- Nguyen, A., & Schulze, H. J. (2003). **Colloidal science of flotation.** CRC press.
- Oldshue, J. Y. (1983). **Fluid mixing technology.**

Parry, T. J. (2008). *I. Thermodynamics and Magnetism of Cu 2 OCl 2 II. Repairs to Microcalorimeter*. Brigham Young University.

Richardson, J. F. (1954). u. WN Zaki: **Sedimentation and fluidization**. *Trans. Instn. chem. Engrs. Bd*, 32, 35.

Ryskamp, J. M., Hildebrandt, P., Baba, O., Ballinger, R., Brodsky, R., Chi, H. W., ... & Lensa, W. V. (2004). **Design Features and Technology Uncertainties for the Next Generation Nuclear Plant (No. INEEL/EXT-04-01816)**. Idaho National Lab.(INL), Idaho Falls, ID (United States).

Serban, M., Lewis, M. A., & Basco, J. K. (2004). **Kinetic study of the hydrogen and oxygen production reactions in the copper-chloride thermochemical cycle**. American Institute of Chemical Engineers.

Trevani, L. (2011, May). **The copper-chloride cycle: synthesis and characterization of copper oxychloride**. In *Hydrogen and Fuel Cells International Conference and Exhibition*.

MARIANA NATALE FIORELLI FABICHE: Graduated in Civil Engineering from Universidade Paranaense (2009-2013), with a specialization in Project Management and Building Works from Universidade Estadual de Maringá (2014-2016). She has a Master's degree in Urban Engineering from the State University of Maringá (2014-2016) and a PhD in Civil Engineering from the State University of Londrina (2018-2023). She worked as an hourly Professor at Universidade Paranaense in the areas of Civil Engineering and Architecture between the years 2017-2022, as well as contributing and participating in the course's board of directors. Currently (2021- Current) she is a professor in the Department of Technology (DTC) in the Civil Engineering and Construction Technology courses at the State University of Maringá Campus de Umuarama, teaching subjects in Thermal Comfort, Hydrology, Hydraulics I, Hydraulic Laboratory I and II, Construction Materials, Construction Management, among others. She participates in research projects and contributes to the development of the respective courses.

B

Borderless education 14

C

Ceramic processing 1, 2, 3, 9, 10

Conduction 24, 28

Cu-Cl cycle 24, 25, 26, 40, 41, 42, 43, 44, 45, 46, 47, 49, 53, 54, 64, 65, 66, 67, 70

D

Decorative pieces 2, 9

E

E-Learning 14, 15, 16, 19, 20, 21, 22

G

Globalization 14, 15, 22

H

Heat balance 24, 26, 38, 40, 51, 54, 55

Heat transfer 24, 26, 27, 28, 29, 30, 31, 33, 34, 35, 36, 37, 40, 41, 42, 43, 46, 47, 51, 53, 54, 55, 56, 57, 60, 61, 63, 64, 65, 66, 67

Helium gas 24, 26, 33, 34, 35, 36, 38, 39, 40, 49, 53, 55, 56, 60, 63

Hybrid university 15

Hydrogen production 24, 26, 27, 28, 35, 37, 38, 39, 40, 41, 42, 43, 44, 45, 48, 51, 53, 63, 65, 66, 67

I

Industrial revolution Cu-Cl cycle 70

M

Materials reuse 70

Metaverse 14, 15, 16, 17, 18, 19, 20, 21, 22

Metaversity 14, 15, 16, 17, 18, 19, 20, 22, 23

Mining activity 1

O

Oxygen production 25, 40, 41, 43, 44, 49, 50, 54, 56, 64, 65, 66, 67, 68

Oxygen reactors 24, 26, 37, 38, 39, 46, 55

R

Recycling 2

Rejects 1, 2

S

Sanitary ware 2, 9

Scale up 44, 46, 47, 49

Slate poder 70

Slate waste 1, 2, 3, 9, 10, 11

Spiral baffled jacket 24, 26, 29, 30, 31, 37

Sustainability 1, 2, 3, 9

T

Thermal resistance 24, 26, 27, 28, 37, 40, 54


Thermochemical production 44


Thermolysis 25, 40, 42, 44, 49, 50, 56, 65, 66

Three-phase oxygen 24, 42, 54, 66

ENGINEERING IN PERSPECTIVE

SCIENCE, TECHNOLOGY
AND INNOVATION

 www.atenaeditora.com.br

 contato@atenaeditora.com.br

 [@atenaeditora](https://www.instagram.com/atenaeditora)

 www.facebook.com/atenaeditora.com.br


Ano 2024

ENGINEERING IN PERSPECTIVE

SCIENCE, TECHNOLOGY
AND INNOVATION

 www.atenaeditora.com.br

 contato@atenaeditora.com.br

 [@atenaeditora](https://www.instagram.com/atenaeditora)

 www.facebook.com/atenaeditora.com.br


Ano 2024